

STABILITY ANALYSIS OF REACTION-DIFFUSION MODELS ON EVOLVING DOMAINS: THE EFFECTS OF CROSS-DIFFUSION

ANOTIDA MADZVAMUSE

School of Mathematical and Physical Sciences
Department of Mathematics
University of Sussex, Pevensey III, 5C15
Falmer, Brighton, BN1 9QH, England, UK

HUSSAINI S. NDAKWO

School of Mathematical and Physical Sciences
Department of Mathematics
University of Sussex
Falmer, Brighton, BN1 9QH, England, UK

RAQUEL BARREIRA

Polytechnic Institute of Setubal
Barreiro School of Technology
Rua Américo da Silva Marinho-Lavradio
2839-001 Barreiro, Portugal

(Communicated by Hirokazu Ninomiya)

ABSTRACT. This article presents stability analytical results of a two component reaction-diffusion system with linear cross-diffusion posed on continuously evolving domains. First the model system is mapped from a continuously evolving domain to a reference stationary frame resulting in a system of partial differential equations with time-dependent coefficients. Second, by employing appropriately asymptotic theory, we derive and prove cross-diffusion-driven instability conditions for the model system for the case of slow, isotropic domain growth. Our analytical results reveal that unlike the restrictive diffusion-driven instability conditions on stationary domains, in the presence of cross-diffusion coupled with domain evolution, it is no longer necessary to enforce cross nor pure kinetic conditions. The restriction to *activator-inhibitor* kinetics to induce pattern formation on a growing biological system is no longer a requirement. Reaction-cross-diffusion models with equal diffusion coefficients in the principal components as well as those of the *short-range inhibition*, *long-range activation* and *activator-activator* form can generate patterns only in the presence of cross-diffusion coupled with domain evolution. To confirm our theoretical findings, detailed parameter spaces are exhibited for the special cases of isotropic exponential, linear and logistic growth profiles. In support of our theoretical predictions, we present evolving or moving finite element solutions exhibiting patterns generated by a *short-range inhibition*, *long-range activation* reaction-diffusion model with linear cross-diffusion in the presence of domain evolution.

2010 *Mathematics Subject Classification*. Primary: 35K55, 35K57, 35K58; Secondary: 37B55, 37C60, 37C75.

Key words and phrases. Reaction-diffusion systems, cross-diffusion, evolving domains, growing domains, cross-diffusion driven instability, *activator-activator* model, *long-range activation*, *short-range inhibition*, evolving finite elements.

1. **Introduction.** Understanding of biological processes during growth development is an unresolved issue in developmental biology that is only starting to be addressed in the last decade. Introducing domain growth into the modelling results in non-autonomous systems of partial differential equations whose analytical tractability is not yet well understood [7, 11, 18, 19, 24]. In the area of developmental biology, partial differential equations for pattern formation take the form of reaction-diffusion type [13, 30, 37]. On stationary domains, for example, it is well known that one major criticism of reaction-diffusion theory for pattern formation is the tight control of the model reaction kinetic parameter values [3]. Underpinning this theory is the concept of *diffusion-driven* instability which leads to patterns that are stationary in time and periodic in space. For a two-component reaction-diffusion system, a key requirement for diffusion-driven instability is the concept of *long-range inhibition* and *short-range activation* [10]. This implies that one of the species (the inhibitor) must diffuse faster (typically much faster) than the autocatalytic species (activator) thereby fulfilling one of the necessary conditions for the formation of spatial structure.

Several generalisations of the reaction-diffusion theory for pattern formation have been undertaken in order to relax some of these constraints. One of these generalisations involve the introduction of domain growth [7, 18, 19, 24]. It is well-known that many problems in biology involve growth. In [24] we proved that in the presence of domain growth, it is no longer necessary to restrict reaction kinetics to an *activator-inhibitor* type; a *long-range activation* and *short-range inhibition/activation* chemical process are all capable of giving rise to what we termed *domain-growth* induced diffusion-driven instability. *However, this generalisation still requires that the inhibitor must diffuse much faster than the activator species and therefore equal diffusion coefficients do not give rise to the formation of spatial structure during growth.*

Another generalisation is the introduction of cross-diffusion. In many multi-component systems, there are various forms of diffusion depending on the biochemical problem at hand [38]. Diffusive processes can be characterised as *self-diffusion*, *cross-diffusion*, *mutual-diffusion*, *tracer-diffusion*, *intra-diffusion*, *inter-diffusion*, *uphill-diffusion* and *negative- or incongruent-diffusion*. A detailed review of the different physicochemical interpretations of these forms of diffusion is given by Vanag and Epstein [38]. Cross-diffusion is characterised by a gradient in the concentration of one species inducing a flux of another chemical species. In molecular biology, cross-diffusion processes appear in multicomponent systems containing at least two solute components [28, 40]. Multicomponent systems containing nanoparticles, surfactants, polymers and other macromolecules in solution play an important role in industrial applications and biological functions [28]. In developmental biology, recent experimental findings demonstrate that cross-diffusion can be quite significant in generating spatial structure [38]. The effects of cross-diffusion on models for pattern formation (i.e. reaction-diffusion type) have been studied in many theoretical papers [5, 6, 8, 9, 12, 14, 33, 34, 36, 41, 42, 43]. Recently, in Madzvamuse [26] we showed that introducing cross-diffusion to a system of reaction-diffusion equations results in further relaxation of the conditions necessary for the emergency of patterns. In particular, an *inhibitor* and *activator* or two *activators* can diffuse at equal rates, however, the product of the rates of the principal diffusion coefficients must be greater than the product of the cross-diffusion rates. For detailed theoretical analytical and computational results on the effects of domain

growth on pattern formation, the interested reader is referred to results published in [7, 11, 15, 16, 17, 19, 24, 27]. In this article our focus is to study, both theoretically and computationally, how cross-diffusion induces patterning in the presence of domain evolution.

Hence, our paper is organised as follows: in Section 2 we present the model equations posed on evolving domains and these consists of a system of reaction-diffusion equations with linear cross-diffusion. Domain evolution terms are modelled through dilution and convective terms. For analytical purposes, in this section, we map at all times, the model system from a continuously evolving domain to a reference frame (which can be taken as the initial domain). As a result, a system of non-autonomous partial differential equations is obtained. The bulk of our work is detailed in Section 3 where we derive and prove the conditions for cross-diffusion driven instability on evolving domains. These conditions are a generalisation of the classical Turing and cross-diffusion driven instability conditions on stationary domains. Cross-diffusion induced parameter spaces are computed and exhibited in Section 4 for the special cases of isotropic exponential, linear and logistic growth profiles. It is in this section that we exhibit several parameter spaces induced by cross-diffusion in the presence of domain evolution. By selecting model parameter values from the cross-diffusion induced parameter spaces, in Section 5, we present finite element solutions on two-dimensional evolving domains demonstrating the emergence of patterns induced by cross-diffusion and domain growth, for the case of the *short-range inhibition, long-range activation*. Such patterns can not be formed in the absence of cross-diffusion. In Section 6, we conclude and discuss the implications of our findings to the theory of pattern formation during planar growth development.

2. Reaction-diffusion systems with linear cross-diffusion posed on evolving domains. Let $\Omega(t) \subset \mathbb{R}^m$ ($m = 1, 2, 3$) be a simply connected bounded evolving volume for all time $t \in I = [0, t_F]$, $t_F > 0$ and $\partial\Omega(t)$ be the evolving boundary enclosing $\Omega(t)$. Also let $\mathbf{u} = (u(\mathbf{x}, t), v(\mathbf{x}, t))^T$ be a vector of two chemical concentrations at position $\mathbf{x} \in \Omega(t) \subset \mathbb{R}^m$. The evolution equations for reaction-diffusion systems with linear cross-diffusion can be obtained from the application of the law of mass conservation in an elemental volume using Reynolds transport theorem. The growth of the volume $\Omega(t)$ generates a flow of velocity \mathbf{V} to yield the non-dimensional system [11, 24, 30]

$$\left\{ \begin{array}{l} \left\{ \begin{array}{l} u_t + \nabla \cdot (\mathbf{V}u) = \nabla^2 u + d_v \nabla^2 v + \gamma f(u, v), \\ v_t + \nabla \cdot (\mathbf{V}v) = d \nabla^2 v + d_u \nabla^2 u + \gamma g(u, v), \end{array} \right. \quad \mathbf{x} \in \Omega(t), t \geq 0, \\ \mathbf{n} \cdot \nabla u = \mathbf{n} \cdot \nabla v = 0, \quad x \text{ on } \partial\Omega(t), t \geq 0, \\ u(\mathbf{x}, 0) = u_0(\mathbf{x}), \text{ and } v(\mathbf{x}, 0) = v_0(\mathbf{x}), \quad \mathbf{x} \text{ on } \Omega(0), \end{array} \right. \quad (1)$$

where ∇^2 is the Laplace operator on domains and volumes, $d = \frac{D_v}{D_u}$ is the ratio of the diffusion coefficients and $d_u = \frac{D_{uv}}{D_u}$ and $d_v = \frac{D_{vu}}{D_v}$ are the ratios of the cross-diffusion, where D_u, D_v, D_{uv} and D_{vu} are dimensional diffusion and cross-diffusion coefficients, respectively. Here, \mathbf{n} is the unit outward normal to $\Omega(t)$. In the above, $\mathbf{V}(\mathbf{x}, t)$ denotes the flow velocity of the chemical species due to domain evolution. Initial conditions are prescribed through non-negative bounded functions $u_0(\mathbf{x})$ and

$v_0(\mathbf{x})$. The functions, $f(u, v)$ and $g(u, v)$ represent nonlinear reactions. Note that we have imposed self-organisation on the system through zero-flux (also known as homogeneous Neumann) boundary conditions.

Remark 1. Domain growth has the effect of introducing extra terms to the classical model of reaction-diffusion with linear cross-diffusion. For example, for the u equation these are of the form

$$\nabla \cdot (\mathbf{V}u) = \mathbf{V} \cdot \nabla u + u(\nabla \cdot \mathbf{V})$$

where $\mathbf{V} \cdot \nabla u$ represents the transport of the chemical species by the flow velocity \mathbf{V} and $u(\nabla \cdot \mathbf{V})$ denotes the dilution (or concentration) of the chemical species due to domain growth (or contraction) if $\nabla \cdot \mathbf{V} > 0$ (or $\nabla \cdot \mathbf{V} < 0$), respectively.

For analytical clarity and simplicity, we will write the model system (1) in compact-vector form as

$$\mathbf{u}_t + \nabla \cdot (\mathbf{a} : \mathbf{u} - \mathbf{D} \nabla \mathbf{u}) = \gamma \mathbf{F}(\mathbf{u}), \tag{2}$$

where

$$\mathbf{u} = \begin{pmatrix} u \\ v \end{pmatrix}, \mathbf{F} = \begin{pmatrix} f(u, v) \\ g(u, v) \end{pmatrix}, \mathbf{a} : \mathbf{u} = \begin{pmatrix} \mathbf{a} u \\ \mathbf{a} v \end{pmatrix}, \text{ and } \mathbf{D} = \begin{pmatrix} 1 & d_v \\ d_u & d \end{pmatrix}.$$

Assumption 2.1 (Flow velocity). *We assume that the flow velocity $\mathbf{V}(\mathbf{x}, t)$ is identical to the domain velocity, i.e.,*

$$\mathbf{V} = \frac{d\mathbf{x}}{dt}$$

as is standard in the derivation of classical reaction-diffusion models on evolving domains on application of the Reynold’s Transport Theorem [1].

Lemma 2.1 (Global existence of solutions of reaction-diffusion systems with cross-diffusion on evolving domains). *Under suitable assumptions on the reaction-kinetics $f(u, v)$ and $g(u, v)$, the diffusion matrix \mathbf{D} and the domain evolution, problem (1) admits a global classical solution.*

Proof. The proof follows directly from Theorem 4.5 in Venkataraman et al., [39] (Theorem 4.5, page 50) under suitable assumptions on the reaction-kinetics $f(u, v)$ and $g(u, v)$, the diffusion matrix \mathbf{D} and the domain evolution. \square

2.2. Mapping to a stationary domain using a Lagrangian transformation.

For analytical convenience we will work with the model system posed on a time-independent domain. Therefore, we introduce a transformation that maps the model system (2) from a continuously evolving planar domain to a time-independent (stationary) domain (see [2, 11, 24] for more details of this approach). In order to do this, without too many technical complications, we will restrict our attention to a special class of domain evolution as detailed in the next section.

Assumption 2.3 (Isotropic domain evolution). *We assume a spatially linear isotropic evolution of the domain $\Omega(t)$ of the form*

$$\mathbf{x} = \varphi(t)\boldsymbol{\xi} \quad \text{for all } \boldsymbol{\xi} \in \Omega(0), \quad t \geq 0 \text{ and all } \mathbf{x} \in \Omega(t), \tag{3}$$

where $\varphi(t)$ is a continuously differentiable function with $\varphi(0) = 1$. In the above, $\boldsymbol{\xi}$ represents the spatial coordinates of the stationary domain. This assumption and Assumption 2.1 imply that

$$\mathbf{V}(\mathbf{x}, t) = \dot{\varphi}(t)\boldsymbol{\xi}, \tag{4}$$

where $\dot{\varphi} := \frac{d\varphi}{dt}$.

Proposition 1. *Assumptions 2.1 and 2.3 imply that the divergence of the flow velocity is given by*

$$h(t) := \nabla \cdot \mathbf{V} = m \frac{\dot{\varphi}(t)}{\varphi(t)}, \quad m \geq 1,$$

where m defines the number of spatial dimensions.

Proof. The proof can be found in [11, 22, 24]. □

We are now in a position to state the reaction-diffusion system with linear cross-diffusion posed on a stationary domain. Assuming uniform isotropic evolution of the domain, we can write

$$\hat{\mathbf{u}}(\boldsymbol{\xi}, t) = \mathbf{u}(\mathbf{x}, t) = \mathbf{u}(\varphi(t)\boldsymbol{\xi}, t), \quad \boldsymbol{\xi} \in \Omega(0), t \geq 0.$$

As a result, model (2) simplifies to

$$\begin{cases} \hat{\mathbf{u}}_t + h(t)\hat{\mathbf{u}} = \frac{1}{\varphi^2(t)}\mathbf{D} \nabla^2 \hat{\mathbf{u}} + \gamma \mathbf{F}(\hat{\mathbf{u}}), & \boldsymbol{\xi} \text{ on } \Omega(0), t > 0, \\ \mathbf{n} \cdot \nabla \hat{\mathbf{u}}(\boldsymbol{\xi}, t) = 0, & \boldsymbol{\xi} \text{ on } \partial\Omega(0), t \geq 0, \\ \hat{\mathbf{u}}(\boldsymbol{\xi}, 0) = \hat{\mathbf{u}}_0(\boldsymbol{\xi}), & \boldsymbol{\xi} \text{ on } \Omega(0), t = 0, \end{cases} \tag{5}$$

where $h(t) := \nabla \cdot \mathbf{V}$.

From here onwards, we will drop the hats $\hat{\cdot}$ for ease of exposition.

2.3.1. Timescales. For a biological system, growth is typically driven by cell division, and thus occurs on the timescale of the cell cycle duration, which is typically 24 hours or greater. In contrast, the biochemical reaction kinetics are typically considered to occur on a much faster time scale of seconds to minutes, and are typically constrained by the diffusive dynamics. The length scale associated with a volume of 10^4 to 10^6 cells is about $2 \times 10^{-4}\text{m}$ to 10^{-3}m . Given diffusion and cross-diffusion coefficients of between $10^{-6}\text{cm}^2\text{s}^{-1}$ to $10^{-5}\text{cm}^2\text{s}^{-1}$, the diffusive and cross-diffusive timescales occur between 40 seconds to 170 minutes [38]. We will take advantage of this difference in timescales in our analysis. With T_g denoting the growth timescale, and T_{dyn} denoting the maximum of the diffusive timescale and the biochemical kinetics timescale, we will define and utilise the small parameter

$$\epsilon \stackrel{\text{def}}{=} \frac{T_{dyn}}{T_g} \ll 1, \tag{6}$$

and therefore we will generally neglect $O(\epsilon^2)$ corrections. Following [24], it can be shown that for the above range of estimates $\epsilon \in [5 \times 10^{-4}, 0.12]$.

3. Analysis of domain-induced cross-diffusion driven instability.

3.1. Definitions. In the following, we carry out cross-diffusion driven instability analysis of a spatially linear, isotropic evolution of the domain. Given that model system (5) is a non-autonomous system of partial differential equations with time-dependent coefficients, the model system does not always admit a uniform steady state. To this end, we will consider a time-dependent manifold (i.e. spatially independent) $\mathbf{u}_S(t)$ defined as follows.

Definition 3.1 (A spatially independent time-dependent manifold). A spatially independent manifold $\mathbf{u}_S(t)$ is a solution of (5) if it solves the non-autonomous system of ordinary differential equations

$$\frac{\partial \mathbf{u}_S}{\partial t} + h(t)\mathbf{u}_S = \gamma \mathbf{F}(\mathbf{u}_S), \text{ for } t > 0, \text{ given } \mathbf{u}_S(0) = \mathbf{u}_S^0 \in \mathbb{R}. \tag{7}$$

Remark 2. In all our numerical examples presented in Sections 4 and 5, initial conditions $\mathbf{u}_S(0)$ are taken as small random perturbations around the uniform steady state $(a + b, \frac{b}{(a+b)^2})$ obtained on stationary domains.

Definition 3.2 (Cross-diffusion driven instability on evolving domains). Cross-diffusion driven instability on evolving domains occurs when a spatially independent manifold $\mathbf{u}_S(t)$, linearly stable in the absence of spatial variations (diffusion and cross-diffusion terms) becomes unstable in the presence of spatial variations.

3.2. Linear stability analysis of the non-autonomous system. To proceed in investigating the possibility of a cross-diffusion driven instability during domain evolution, we will work with a Lagrangian coordinate system and expand $\mathbf{u}(\boldsymbol{\xi}, t)$ about the spatially independent solution $\mathbf{u}_S(t)$. Thus we substitute

$$\mathbf{u}(\boldsymbol{\xi}, t) = \mathbf{u}_S(t) + \eta \mathbf{w}(\boldsymbol{\xi}, t), \quad \text{with } \eta \ll 1,$$

into the model system (5), where the components of \mathbf{w} are denoted by $(u_*(\boldsymbol{\xi}, t), w_*(\boldsymbol{\xi}, t))^T$. On neglect of $O(\eta^2)$ and higher order terms we obtain the following linearised non-autonomous system of reaction-diffusion equations with linear cross-diffusion

$$\begin{cases} \mathbf{w}_t + h(t)\mathbf{w} = \frac{1}{\varphi^2(t)} \mathbf{D} \nabla^2 \mathbf{w} + \gamma \mathbf{J}_{\mathbf{F}} \Big|_{\mathbf{u}_S} \mathbf{w}, \boldsymbol{\xi} \text{ on } \Omega(0), t > 0, \\ \mathbf{n} \cdot \nabla \mathbf{w}(\boldsymbol{\xi}, t) = 0, \boldsymbol{\xi} \text{ on } \partial\Omega(0), t \geq 0, \\ \mathbf{w}(\boldsymbol{\xi}, 0) = \mathbf{w}_0(\boldsymbol{\xi}), \boldsymbol{\xi} \text{ on } \Omega(0), t = 0. \end{cases} \tag{8}$$

In the above, $\mathbf{J}_{\mathbf{F}}(t)$ is the Jacobian matrix corresponding to the linearisation of the non-linear reaction kinetics which is evaluated at $\mathbf{u}_S(t)$. We define $\psi_K(\boldsymbol{\xi})$ to be the time-independent eigenmode of the transport operator satisfying

$$\begin{cases} \nabla^2 \psi_K = -K^2 \psi_K, \boldsymbol{\xi} \in \Omega(0), \\ \mathbf{n} \cdot \nabla \psi_K(\boldsymbol{\xi}) = 0, \boldsymbol{\xi} \text{ on } \partial\Omega(0). \end{cases} \tag{9}$$

A standard analysis shows that the eigenvalue must be real and negative, and thus without loss of generality, we write it as $-K^2$ in the above. We similarly have that eigenmodes of distinct eigenvalues are orthogonal. Furthermore, we note that the domain $\Omega(0)$ is time-independent because $\boldsymbol{\xi}$ is a Lagrangian coordinate system.

We proceed by expanding \mathbf{w} in terms of the eigenmodes

$$\mathbf{w}(\boldsymbol{\xi}, t) = \sum_K \mathbf{w}_K(\boldsymbol{\xi}, t) = \sum_K \boldsymbol{\beta}_K(t) \psi_K(\boldsymbol{\xi}). \tag{10}$$

Linearity and the orthogonality of the eigenmodes allow each mode to be considered separately, which is a substantial simplification. In particular, growth of any one of the $\boldsymbol{\beta}_K(t)$ with time is sufficient to drive the full solution away from the time-dependent solution $\mathbf{u}_S(t)$. Similarly, if all the $\boldsymbol{\beta}_K(t)$ decay with time then a

sufficiently small perturbation from the time-dependent solution $\mathbf{u}_S(t)$ will decay, at least within the resolution of linear theory predictions.

To proceed, we substitute, for each K , a mode $\mathbf{w}_K = \boldsymbol{\beta}_K(t)\psi_K(\boldsymbol{\xi})$ from expansion (10) into the linearised equation (8) to find

$$\left[\left(\dot{\boldsymbol{\beta}}_K + h(t)\boldsymbol{\beta}_K \right) + \frac{K^2}{\varphi^2(t)} \mathbf{D}\boldsymbol{\beta}_K - \gamma \mathbf{J}_{\mathbf{F}}(t)|_{\mathbf{u}_S} \boldsymbol{\beta}_K \right] \psi_K = \mathbf{0}. \tag{11}$$

Writing

$$\boldsymbol{\beta}_K(t) = \mathbf{b}_K(t)q(t),$$

where $q(t) = \exp \left[- \int_{t_0}^t h(\tau) d\tau \right]$ and t_0 is the point the perturbation is applied, we have

$$\left[\dot{\mathbf{b}}_K + \frac{K^2}{\varphi^2(t)} \mathbf{D}\mathbf{b}_K - \gamma \mathbf{J}_{\mathbf{F}}(t)|_{\mathbf{u}_S} \mathbf{b}_K \right] \psi_K q(t) = \mathbf{0}. \tag{12}$$

One can immediately deduce that

$$\frac{d\mathbf{b}_K}{dt} = \mathbf{M}_K(t)\mathbf{b}_K, \text{ where } \mathbf{M}_K(t) \stackrel{def}{=} \left[- \frac{K^2}{\varphi^2(t)} \mathbf{D} + \gamma \mathbf{J}_{\mathbf{F}}(t)|_{\mathbf{u}_S} \right]. \tag{13}$$

Given initial conditions, $\mathbf{b}_K(t_0)$ at time t_0 we seek a solution at time $t > t_0$ of the form

$$\mathbf{b}_K(t) = \exp \left[\int_{t_0}^t ds \lambda_K^*(s) \right] \mathbf{c}_K(t), \tag{14}$$

where $\lambda_K^*(t)$ is either the largest time-dependent real eigenvalue of $\mathbf{M}_K(t)$ or the real part of one of the time-dependent complex conjugate eigenvalues. From equations (13) and (14) we have

$$\frac{d\mathbf{c}_K}{dt} = \mathbf{Q}_K(t)\mathbf{c}_K, \text{ where } \mathbf{Q}_K(t) \stackrel{def}{=} \left[\mathbf{M}_K(t) - \lambda_K^*(t)\mathbf{I} \right], \tag{15}$$

with $\mathbf{c}_K(t_0) = \mathbf{b}_K(t_0)$.

3.3. Analysis of solutions of non-autonomous systems of ordinary differential equations. The analysis of the solutions of the non-autonomous systems of ordinary differential equations is identical to that derived and presented in Madzvamuse *et al.*, [24]. The only difference now is the inclusion of the cross-diffusion coefficients into the matrix $\mathbf{M}_K(t)$. We present a summary of the analysis for completeness' sake, the reader is referred to [24] for further details. First, we observe that for a matrix \mathbf{Q} , the induced matrix norm is defined as

$$\|\mathbf{Q}\| = \sup_{\|\mathbf{x}\|=1} \|\mathbf{Q}\mathbf{x}\|$$

and the Lozinskii measure is [29]

$$\mu(\mathbf{Q}) = \lim_{h \rightarrow 0} \frac{\|\mathbf{I} + h\mathbf{Q}\| - 1}{h}.$$

It can be easily shown that $\|\mathbf{Q}\mathbf{x}\| \leq \|\mathbf{Q}\| \|\mathbf{x}\|$, for any matrix \mathbf{Q} and vector \mathbf{x} .

Proposition 2. *Assume that $\mathbf{M}_K(t)$ has real and distinct eigenvalues, then*

$$\frac{\|\mathbf{b}_K(t_0 + \Delta t)\|}{\|\mathbf{b}_K(t_0)\|} = \exp \left[\lambda_K^* \left(t_0 + \frac{\Delta t}{2} \right) \Delta t \right] [1 + O(\epsilon^2)], \tag{16}$$

with λ_K^* the largest real eigenvalue of \mathbf{M}_K .

Proof. First, we prove that $\mathbf{c}_K(t)$ is bounded from above. The matrix $\mathbf{Q}_K(t)$ possesses one zero and one negative eigenvalue. Let us denote by $\mathbf{e}_K^0(t)$ the unit eigenvector associated with the zero eigenvalue and let $\mathbf{e}_K^1(t)$ be the unit eigenvector associated with the negative eigenvalue, such that the angle between $\mathbf{e}_K^0(t)$ and $\mathbf{e}_K^1(t)$ is acute. These eigenvectors are distinct and are linearly independent and thus form a spanning set. Hence we can write

$$\mathbf{c}_K(t) = \alpha_K(t)\mathbf{e}_K^0(t) + \beta_K(t)\mathbf{e}_K^1(t), \quad \text{and} \quad \|\mathbf{c}_K(t)\| = \sqrt{\alpha_K^2(t) + \beta_K^2(t)}.$$

The above satisfies all the axioms required of a norm. It then follows that

$$\begin{aligned} \frac{d}{dt}\|\mathbf{c}_K(t)\| &= \lim_{h \rightarrow 0} \frac{\|\mathbf{c}_K(t+h)\| - \|\mathbf{c}_K(t)\|}{h} \\ &= \lim_{h \rightarrow 0} \frac{\|\mathbf{c}_K(t) + h\mathbf{Q}_K(t)\mathbf{c}_K(t)\| - \|\mathbf{c}_K(t)\|}{h} \\ &\leq \lim_{h \rightarrow 0} \frac{\|\mathbf{I} + h\mathbf{Q}_K(t)\| \|\mathbf{c}_K(t)\| - \|\mathbf{c}_K(t)\|}{h} \\ &= \mu(\mathbf{Q}_K(t))\|\mathbf{c}_K(t)\|. \end{aligned}$$

Hence

$$\|\mathbf{c}_K(t)\| \leq \|\mathbf{c}_K(t_0)\| \exp \left[\int_{t_0}^t ds \mu(\mathbf{Q}_K(s)) \right] = \|\mathbf{c}_K(t_0)\|,$$

noting that a matrix with zero and negative eigenvalues has a zero Lozinskii measure. Thus a solution to equation (15) does not grow in time.

Next, we prove that $\mathbf{c}_K(t)$ does not decay to zero. Taking t fixed, with $\Delta t = t - t_0 \sim T_{dyn}$, we can find at least one solution of (15) which does not decay on neglecting $O(\epsilon^2)$ corrections. From a Picard iteration we have

$$\mathbf{c}_K(t) = \mathbf{G}_K(t, t_0)\mathbf{c}_K(t_0), \tag{17}$$

where

$$\mathbf{G}_K(t, t_0) = \mathbf{I} + \sum_{n=1}^{\infty} \int_{t_0}^t dt_1 \int_{t_0}^{t_1} dt_2 \cdots \int_{t_0}^{t_{n-1}} dt_n \mathbf{Q}_K(t_1)\mathbf{Q}_K(t_2) \cdots \mathbf{Q}_K(t_n). \tag{18}$$

The existence of $\mathbf{G}_K(t, t_0)$ is guaranteed from Picard’s theorem given the components of $\mathbf{Q}_K(t)$ are bounded to ensure that $\mathbf{Q}_K(t)\mathbf{c}_K(t)$ is Lipschitz. With “dot” denoting a time derivative, we have

$$\dot{\mathbf{Q}}_K \sim O\left(\frac{1}{T_{growth}}\mathbf{Q}_K\right) \sim O\left(\frac{\epsilon}{T_{dyn}}\mathbf{Q}_K\right)$$

since the change in the matrix \mathbf{Q} is driven by growth. We set the initial condition $\mathbf{c}_K(t_0) = \mathbf{e}_K^0(t_0)$ and consider the solution (17) obtained by expanding each $\mathbf{Q}_K(t)$ in expression (18). Noting $\mathbf{Q}_K(t_0)\mathbf{e}_K^0(t_0)$ is zero and that the n^{th} order time derivatives of $\mathbf{Q}_K(t)$ scale with ϵ^n , we have

$$\mathbf{c}_K(t) = \mathbf{e}_K^0(t_0) + \sum_{n=1}^{\infty} \frac{\Delta t^{n+1}}{(n+1)!} \mathbf{Q}_K^{n-1}(t_0)\dot{\mathbf{Q}}_K(t_0)\mathbf{e}_K^0(t_0) + O(\epsilon^2). \tag{19}$$

By differentiating $\mathbf{Q}_K(s)\mathbf{e}_K^0(s) = 0$ with respect to s and then setting $s = t_0$ we have

$$\dot{\mathbf{Q}}_K(t_0)\mathbf{e}_K^0(t_0) = -\mathbf{Q}_K(t_0)\dot{\mathbf{e}}_K^0(t_0).$$

Let $\mathbf{e}_K^{0P}(t)$ be the unit vector which is perpendicular to $\mathbf{e}_K^0(t)$ where P denotes perpendicular. Because $\mathbf{e}_K^0(t)$ is defined to be a unit vector, we have

$$\dot{\mathbf{e}}_K^0(t) = \frac{\epsilon}{\tau(t)} \mathbf{e}_K^{0P}(t);$$

where $\tau(t)$ has an implicit K dependence. Since the matrix $\mathbf{Q}_K(t)$ changes on the growth timescale we also have that $\epsilon/\tau(t) \sim O(T_{growth}^{-1})$ and hence $\tau(t) \sim O(T_{dyn})$. We also have the kinematic relation

$$\mathbf{e}_K^1(t) = \cos \psi(t) \mathbf{e}_K^{0P}(t) + \sin \psi(t) \mathbf{e}_K^0(t) \tag{20}$$

by projecting $\mathbf{e}_K^1(t)$ onto the $\mathbf{e}_K^0(t)$ and $\mathbf{e}_K^{0P}(t)$ directions. Note that $\psi(t)$ has an implicit K dependence and that, without loss of generality, $\psi(t) \in [0, \pi/2)$. Hence

$$\mathbf{Q}_K(t_0) \dot{\mathbf{e}}_K^0(t_0) = \frac{\lambda_K^0(t_0)}{\tau(t_0) \cos \psi(t_0)} \mathbf{e}_K^1(t),$$

where $\lambda_K^0(t_0) < 0$ is the negative eigenvalue of $\mathbf{Q}_K(t_0)$. By substituting this into equation (19) we have

$$\begin{aligned} \mathbf{c}_K(t) &= [1 + O(\epsilon^2)] \mathbf{e}_K^0(t_0) + \tag{21} \\ &\left[\frac{\epsilon \Delta t}{\tau(t_0) \cos \psi(t_0)} \left(\frac{e^s - (1 + s)}{s} \right) \Big|_{s=\lambda_K^0(t_0)\Delta t} + O(\epsilon^2) \right] \mathbf{e}_K^1(t_0) \end{aligned}$$

which is not decaying.

From equations (14), (21) and the observation that

$$\begin{aligned} \int_{t_0}^{t_0+\Delta t} ds \lambda_K^*(s) &= \lambda_K^* \left(t_0 + \frac{\Delta t}{2} \right) \Delta t + \ddot{\lambda}_K^* \left(t_0 + \frac{\Delta t}{2} \right) \\ &\quad \times \int_{t_0}^{t_0+\Delta t} ds \left(s - \left[t_0 + \frac{\Delta t}{2} \right] \right) + \dots \\ &\approx \lambda_K^* \left(t_0 + \frac{\Delta t}{2} \right) \Delta t \left[1 + O \left(\frac{\epsilon^2 \Delta t^2}{T_{dyn}^2} \right) \right] \end{aligned}$$

where we have used the scaling relation $\ddot{\lambda}_K^* \sim O(\epsilon^2 \lambda_K^*/T_{dyn}^2)$, it can be easily shown that

$$\frac{\|\mathbf{b}_K(t_0 + \Delta t)\|}{\|\mathbf{b}_K(t_0)\|} = \exp \left[\lambda_K^* \left(t_0 + \frac{\Delta t}{2} \right) \Delta t \right] [1 + O(\epsilon^2)], \tag{22}$$

with λ_K^* the largest real eigenvalue of \mathbf{M}_K . □

Proposition 3. *Assume that $\mathbf{M}_K(t)$ has complex conjugate eigenvalues, then*

$$\frac{\|\mathbf{b}_K(t_0 + \Delta t)\|}{\|\mathbf{b}_K(t_0)\|} = \exp \left[\Delta t \left\{ \lambda_K^* \left(t_0 + \frac{\Delta t}{2} \right) + \epsilon |\hat{B}_K(t_0)| \hat{C}(\Omega_K \Delta t, \chi_1) \right\} \right]$$

with

$$\begin{aligned} \hat{C}(\Omega_K \Delta t, \chi_1) &: \stackrel{def}{=} \left[1 - 2 \cos(\Omega_K \Delta t) \frac{\sin(\Omega_K \Delta t)}{\Omega_K \Delta t} + \frac{\sin^2(\Omega_K \Delta t)}{[\Omega_K \Delta t]^2} \right]^{1/2} \\ &\times \cos(\Omega_K \Delta t + \chi_1); \end{aligned}$$

where $\Omega_K : \stackrel{def}{=} \text{Im}(\lambda(t)) > 0$ and \hat{B}_K is evaluated at time t_0 .

Proof. Let

$$\mathbf{e}_K(t) = \mathbf{f}_K^0(t) + i\mathbf{f}_K^1(t)$$

be a complex eigenvector of the matrix $\mathbf{M}_K(t)$ whose associated complex eigenvalue is given by $\lambda(t)$, where $\mathbf{f}_K^0(t)$, $\mathbf{f}_K^1(t)$ are real, distinct, vectors and thus a spanning set of the real plane. Without loss of generality we take $\mathbf{f}_K^0(t)$ to be a unit vector and let $\Omega_K \stackrel{def}{=} \text{Im}(\lambda(t)) > 0$. We can write any real vector function of time in the form

$$\mathbf{c}_K(t) = \alpha_K(t)\mathbf{f}_K^0(t) + \beta_K(t)\mathbf{f}_K^1(t)$$

and define the norm

$$\|\mathbf{c}_K(t)\| = \sqrt{\alpha_K^2(t) + \beta_K^2(t)}.$$

Following [24] let $\bar{\mathbf{e}}_K(t)$ denotes the conjugate of $\mathbf{e}_K(t)$ then we can write

$$\begin{aligned} \dot{\mathbf{e}}_K(t) &= \dot{\mathbf{f}}_K^0(t) + i\dot{\mathbf{f}}_K^1(t) \stackrel{def}{=} \epsilon A_K \mathbf{f}_K^0(t) + i\epsilon B_K \mathbf{f}_K^1(t) \\ &= \epsilon \frac{A_K + B_K}{2} \mathbf{e}_K(t) + \epsilon \frac{A_K - B_K}{2} \bar{\mathbf{e}}_K(t) \stackrel{def}{=} \epsilon \hat{A}_K \mathbf{e}_K(t) + \epsilon \hat{B}_K \bar{\mathbf{e}}_K(t). \end{aligned} \quad (23)$$

where A_K , B_K , \hat{A}_K , \hat{B}_K are defined by the above relations and are time-dependent. The ϵ appears as the change in the eigenvector $\mathbf{e}_K(t)$ is on the timescale of growth. As long as the angle between \mathbf{f}_K^0 and \mathbf{f}_K^1 is significantly greater than ϵ and the vectors have a ratio of lengths, l , with $\epsilon \ll l \ll \epsilon^{-1}$, then $A_K(t)$ and $B_K(t)$ can be treated as $O(\epsilon^0)$ terms for the purposes of asymptotic expansions. This is assumed below.

We also have that

$$\mathbf{Q}_K(t)\mathbf{e}_K(t) = i\Omega_K \mathbf{e}_K(t), \quad \mathbf{Q}_K(t)\bar{\mathbf{e}}(t) = -i\Omega_K \bar{\mathbf{e}}(t)$$

and hence, by differentiation,

$$\begin{aligned} \dot{\mathbf{Q}}_K(t)\mathbf{e}_K(t) &= -(\mathbf{Q}_K(t) - i\Omega_K \mathbf{I}) \dot{\mathbf{e}}_K(t) + i\dot{\Omega}_K \mathbf{e}_K(t) \\ &= i\epsilon \Omega_K \left[2\hat{B}_K \bar{\mathbf{e}}_K(t) + \Phi_K \mathbf{e}_K(t) \right], \end{aligned}$$

where $\Phi_K \stackrel{def}{=} \dot{\Omega}_K / [\epsilon \Omega_K] \sim O(1/T_{dyn})$ as Ω_K changes on the growth timescale $T_{growth} = T_{dyn}/\epsilon$. Thus for a general initial condition

$$\mathbf{c}_K(t_0) = \alpha_K \mathbf{f}_K^0(t_0) + \beta_K \mathbf{f}_K^1(t_0) = \text{Re} [(\alpha_K - i\beta_K) \mathbf{e}_K(t_0)]$$

we have

$$\begin{aligned} \mathbf{c}_K(t) &= \text{Re} \left[(\alpha_K - i\beta_K) \left\{ \exp[\mathbf{Q}_K(t_0)\Delta t] \mathbf{e}_K(t_0) + \right. \right. \\ &\quad \left. \sum_{n=1}^{\infty} \sum_{j=1}^n \int_{t_0}^t dt_1 \int_{t_0}^{t_1} dt_2 \dots \right. \\ &\quad \left. \left. \int_{t_0}^{t_{n-2}} dt_{n-1} \int_{t_0}^{t_{n-1}} dt_n (t_j - t_0) \mathbf{Q}_K^{j-1}(t_0) \dot{\mathbf{Q}}_K(t_0) \mathbf{Q}_K^{n-j}(t_0) \mathbf{e}_K(t_0) \right\} \right] \\ &\quad + O(\epsilon^2) \\ &= \text{Re} \left[(\alpha_K - i\beta_K) \left\{ \exp[\mathbf{Q}_K(t_0)\Delta t] \mathbf{e}_K(t_0) + \right. \right. \end{aligned}$$

$$\begin{aligned} & \epsilon \sum_{n=1}^{\infty} \sum_{j=1}^n \frac{\Delta t^{n+1}}{(n+1)!} [n-j+1] (i\Omega_K)^n \left[\Phi_K \mathbf{e}_K(t_0) + 2\hat{B}_K (-1)^{j-1} \bar{\mathbf{e}}_K(t_0) \right] \Big\} \\ & + O(\epsilon^2). \\ & = \operatorname{Re} \left[(\alpha_K - i\beta_K) \times \right. \\ & \left. \left\{ e^{i\Omega_K \Delta t} \left\{ 1 + i\epsilon \frac{\Delta t^2}{2} \Phi_K \Omega_K \right\} \mathbf{e}_K(t_0) - \epsilon \hat{B}_K \left\{ \frac{\sin(\Omega_K \Delta t)}{\Omega_K} - \Delta t e^{i\Omega_K \Delta t} \right\} \bar{\mathbf{e}}_K(t_0) \right\} \right] \\ & + O(\epsilon^2). \end{aligned}$$

Calculating the norm reveals

$$\begin{aligned} \|\mathbf{c}_K(t)\|^2 &= \|\mathbf{c}_K(t_0)\|^2 \times \\ & \left\{ 1 + 2\epsilon |\hat{B}_K| \Delta t \left[-\cos(2\Omega_K \Delta t + \chi_0) + \frac{\sin(\Omega_K \Delta t)}{\Omega_K \Delta t} \cos(\Omega_K \Delta t + \chi_0) \right] \right\} \\ & + O(\epsilon^2), \end{aligned}$$

where

$$\chi_0 = \tan^{-1} \left(\frac{2\alpha_K \beta_K \operatorname{Re} \hat{B}_K + (\beta_K^2 - \alpha_K^2) \operatorname{Im} \hat{B}_K}{(\beta_K^2 - \alpha_K^2) \operatorname{Re} \hat{B}_K - 2\alpha_K \beta_K \operatorname{Im} \hat{B}_K} \right) = \arg \left((\alpha_K - i\beta_K)^2 \hat{B}_K \right)$$

is a phase angle. We can rewrite the above norm in the form

$$\begin{aligned} \|\mathbf{c}_K(t)\| &= \|\mathbf{c}_K(t_0)\| \times \\ & \left\{ 1 + \epsilon |\hat{B}_K| \Delta t \left[1 - 2 \cos(\Omega_K \Delta t) \frac{\sin(\Omega_K \Delta t)}{\Omega_K \Delta t} + \frac{\sin^2(\Omega_K \Delta t)}{[\Omega_K \Delta t]^2} \right]^{1/2} \cos(\Omega_K \Delta t + \chi_1) \right\} \\ & + O(\epsilon^2), \end{aligned}$$

where

$$\chi_1 = \chi_0 + \tan^{-1} \left(\frac{\sin(\Omega_K \Delta t)}{\cos(\Omega_K \Delta t) - \frac{\sin(\Omega_K \Delta t)}{\Omega_K \Delta t}} \right).$$

Thus we have an oscillating solution, the amplitude of which is constant at leading order but not at higher orders. One can immediately deduce that, accurate to $O(\epsilon^2)$

$$\frac{\|\mathbf{b}_K(t_0 + \Delta t)\|}{\|\mathbf{b}_K(t_0)\|} = \exp \left[\Delta t \left\{ \lambda_K^* \left(t_0 + \frac{\Delta t}{2} \right) + \epsilon |\hat{B}_K(t_0)| \hat{C}(\Omega_K \Delta t, \chi_1) \right\} \right]$$

with

$$\hat{C}(\Omega_K \Delta t, \chi_1) \stackrel{def}{=} \left[1 - 2 \cos(\Omega_K \Delta t) \frac{\sin(\Omega_K \Delta t)}{\Omega_K \Delta t} + \frac{\sin^2(\Omega_K \Delta t)}{[\Omega_K \Delta t]^2} \right]^{1/2} \cos(\Omega_K \Delta t + \chi_1);$$

note that \hat{B}_K is evaluated at time t_0 . □

Lemma 3.3. *The important result for investigating stability is that an $O(\epsilon^2)$ accurate estimate of the growth rate between time t_0 and time t is given by*

$$\begin{aligned} \lambda_K^G &\stackrel{def}{=} \lambda_K^* \left(t_0 + \frac{\Delta t}{2} \right) \\ &+ \epsilon \left\{ |\hat{B}_K(t_0)| \left[1 - 2 \cos(\Omega_K \Delta t) \frac{\sin(\Omega_K \Delta t)}{\Omega_K \Delta t} + \frac{\sin^2(\Omega_K \Delta t)}{\Omega_K^2 \Delta t^2} \right]^{1/2} \right. \\ &\left. \times \cos(\Omega_K \Delta t + \chi_1) \right\} \end{aligned}$$

with λ_K^* denoting the real part of the eigenvalues of M_K .

Remark 3. The case when the matrix $M_K(t)$ has real, repeated eigenvalues requires a mathematically precise parameter fine tuning, and thus is unlikely to occur in most models which is inappropriate for biological models.

3.4. Cross-diffusion driven instability conditions on evolving domains.

Following Madzvamuse *et al.*, [24], we consider a perturbation at time t_0 , which can be distinct from the initial time, and how it has evolved by time $t = t_0 + \Delta t > t_0$ with $\frac{\Delta t}{T_{dyn}} \sim O(\epsilon^0)$ where ϵ is defined in section (2.3.1). We are now in a position to state the conditions for cross-diffusion driven instability. For this, it will be useful to define $t_1 \stackrel{def}{=} \frac{t_0+t}{2}$ for use below.

Theorem 3.4. *The necessary conditions for a cross-diffusion driven instability (accurate to first order in $\epsilon \ll 1$) when considering the system at time t due to a perturbation at time $t_0 < t$ in the presence of spatially linear and isotropic growth as in system (5), are given by*

$$\gamma(f_u + g_v) - 2h_* < 0, \tag{24}$$

$$\gamma^2(f_u g_v - f_v g_u) - h_* \gamma(f_u + g_v) > 0, \tag{25}$$

$$d - d_u d_v > 0, \tag{26}$$

$$h_*(1 + d) - \gamma(df_u + g_v - d_u f_v - d_v g_u) < 0, \tag{27}$$

$$\begin{aligned} &\left[h_*(1 + d) - \gamma(df_u + g_v - d_u f_v - d_v g_u) \right]^2 \\ &- 4(d - d_u d_v) \left[\gamma^2(f_u g_v - f_v g_u) - \gamma h_*(f_u + g_v) \right] > 0. \tag{28} \end{aligned}$$

In the above, the subscripts u, v denote partial differentiation, with the Jacobian components f_u, f_v, g_u and g_v evaluated in terms of $\mathbf{u}_S(t_1)$. Strictly, we have $h_* \sim O(\epsilon)$, due to the fact that the growth timescale is much longer than any other timescale so that one may self-consistently neglect $O(h_*^2)$ corrections in the above.

Proof. Let $\lambda_K^*(t_1)$ be the largest real part of any eigenvalue of $M_K(t_1)$, $\lambda_k(t_1)$ which is the root of the quadratic equation

$$\det \left[\mathbf{I} \lambda_K^*(t_1) + \frac{K^2}{\varphi^2(t_1)} \mathbf{D} - \gamma \mathbf{J}_F |_{\mathbf{u}_s(t_1)} \right] = 0. \tag{29}$$

Thus, $\lambda_K(t_1)$ satisfies the dispersion relation

$$\lambda_K^2(t_1) + b(K_*^2) \lambda_K(t_1) + c(K_*^2) = 0, \tag{30}$$

where

$$K_*^2 \stackrel{def}{=} \frac{K^2}{\varphi^2(t_1)}, \tag{31}$$

$$b(K_*^2) = K_*^2(1 + d) - \gamma(f_u + g_v), \tag{32}$$

$$c(K_*^2) = (d - d_u d_v)K_*^4 - \gamma K_*^2(df_u + g_v - d_v g_u - d_u f_v) + \gamma^2(f_u g_v - f_v g_u), \tag{33}$$

with $u, v, f(u, v), g(u, v)$ the scalar variables and kinetic functions. The partial derivatives are evaluated in terms of $\mathbf{u}_s(t_1)$ the solution to the non-autonomous system of ordinary differential equations given by (7) at time t_1 .

Let us define the eigenvalue

$$\mu_K \stackrel{def}{=} \lambda_K(t) - h_*$$

corresponding to the eigenfunction $\mathbf{w}_K(\boldsymbol{\xi}, t)$. At time $t_1 = (t_0 + t)/2$ defined above, it follows that the $\mathbf{w}_K(\boldsymbol{\xi}, t_1)$, will grow during the interval $[t_0, t]$ if

$$\mu_K^* \stackrel{def}{=} \lambda_K^*(t_1) - h_* > 0,$$

and will decay if

$$\mu_K^* \stackrel{def}{=} \lambda_K^*(t_1) - h_* < 0.$$

Substituting $\lambda_K(t) = \mu_K + h_*$ into (30) we have

$$\mu_K^2 + (2h_* + b(K_*^2)) \mu_K + (c(K_*^2) + b(K_*^2)h_* + O(h_*^2)) = 0, \tag{34}$$

where $b(K_*^2)$ and $c(K_*^2)$ are given in equations (32) and (33), respectively. For convenience's sake, denoting by $b_{h_*}(K_*^2) = 2h_* + b(K_*^2)$ and $c_{h_*}(K_*^2) = c(K_*^2) + b(K_*^2)h_* + O(h_*^2)$, we obtain the characteristic equation

$$\mu_K^2 + b_{h_*}(K_*^2)\mu_K + c_{h_*}(K_*^2) = 0. \tag{35}$$

Thus

$$2\mu_K = -b_{h_*}(K_*^2) \pm \sqrt{b_{h_*}^2(K_*^2) - 4c_{h_*}(K_*^2)}. \tag{36}$$

Taking $K_* = 0$ we have the absence spatial variations and thus spatial homogeneity. In the absence of spatial variations, we require $\mathbf{u}_s(t_1)$ to be asymptotically stable to the $K_* = 0$ and this is guaranteed provided

$$\mu_K^* = \text{Re}[\mu_K] = \text{Re} \left[-b_{h_*}(0) \pm \sqrt{b_{h_*}^2(0) - 4c_{h_*}(0)} \right] < 0. \tag{37}$$

This is guaranteed provided $b_{h_*}(0) > 0$ and $c_{h_*}(0) > 0$ if and only if the following conditions hold

$$\gamma(f_u + g_v) - 2h_* < 0, \tag{38}$$

$$O(h_*^2) + \gamma^2(f_u g_v - f_v g_u) - h_* \gamma(f_u + g_v) > 0. \tag{39}$$

These first two conditions are domain-induced, and do not reflect the spatial variations as expected. The conditions enforce the requirement that the time-dependent manifold $\mathbf{u}_s(t)$ is asymptotically stable with respect to spatially homogeneous perturbations.

Now, in the presence of spatial variations which includes both diffusion and cross-diffusion, ($K_*^2 > 0$), we have

$$b_{h_*}(K_*^2) = 2h_* + b(K_*^2) = K_*^2(1 + d) + b_{h_*}(0) > 0 \tag{40}$$

since $b_{h_*}(0) > 0$. For $(\mathbf{u}_s(t_1))$ to become unstable, we require that

$$\mu_K^* = \text{Re}[\mu_K] > 0 \quad \text{for some } K_*^2 \text{ non-zero}, \tag{41}$$

thereby requiring that $c_{h_*}(K_*^2) < 0$ for some K_*^2 non-zero. By definition of $c_{h_*}(K_*^2)$ we can further re-arrange to obtain a quadratic polynomial in K_*^2 of the form

$$c_{h_*}(K_*^2) = P_2 K_*^4 + P_1 K_*^2 + c_{h_*}(0) \tag{42}$$

where

$$\begin{aligned} P_2 &= d - d_u d_v, \\ P_1 &= h_*(1 + d) - \gamma(df_u + g_v - d_v g_u - d_u f_v), \\ c_{h_*}(0) &= c(0) + b(0)h_* + O(h_*^2) = \gamma^2(f_u g_v - f_v g_u) - \gamma h_*(f_u + g_v) + O(h_*^2). \end{aligned}$$

Geometrically, $c_{h_*}(K_*^2)$ represents a parabola. For the reaction-diffusion system with cross-diffusion to be well-posed, we require that

$$d - d_u d_v > 0, \tag{43}$$

which implies that the parabola opens upwards. This results in the third condition for cross-diffusion driven instability.

It can be easily shown that $c_{h_*}(K_*^2)$ has a minimum value which is negative provided

$$\begin{aligned} c_{h_*}^{min}(K_{*min}^2) < 0 &\iff \left[h_*(1 + d) - \gamma(df_u + g_v - d_u f_v - d_v g_u) \right]^2 \\ &\quad - 4(d - d_u d_v) \left[\gamma^2(f_u g_v - f_v g_u) - \gamma h_*(f_u + g_v) + O(h_*^2) \right] > 0, \end{aligned} \tag{44}$$

where

$$\begin{aligned} K_{*min}^2 &= \frac{h_*(1 + d) - \gamma(df_u + g_v - d_u f_v - d_v g_u)}{2(d - d_u d_v)} > 0 \\ &\iff h_*(1 + d) - \gamma(df_u + g_v - d_u f_v - d_v g_u) > 0. \end{aligned}$$

In all the above, ignoring $O(h_*^2)$ results in the five conditions for cross-diffusion driven instability conditions (24)-(28). \square

Remark 4. In addition to inequalities (24)-(28), a cross-diffusion driven instability requires that there exists at least one wavenumber such that K_*^2 is contained in the interval

$$K_*^2 \in (K_-^2, K_+^2)$$

where K_{\pm}^2 are the roots of $c_{h_*}(K_{\pm}^2) = 0$ and these are given by

$$K_{\pm}^2 = \frac{-P_1 \pm \sqrt{P_1^2 - 4c_{h_*}(0)(d - d_u d_v)}}{2(d - d_u d_v)}. \tag{45}$$

Remark 5. The inequalities (24)-(28) define a time-dependent domain in parameter space, generalising the cross-diffusion driven instability conditions on stationary domains [25, 26]. On evolving domains, this generalised parameter space is contingent on domain evolution.

3.4.1. *Implications of cross-diffusion on the theory of diffusion-driven instability on evolving domains.* In previous studies [25, 26] we detailed the implications of cross-diffusion to the theory of pattern formation on stationary domains. Those conditions are inherited by the current model on evolving domains. Our focus now is to see if other non-standard reaction kinetics can give rise to cross-diffusion driven instability only in the presence of domain evolution.

1. *In contrast to the autonomous case*, if we have an activator and an inhibitor, we do not require *short-range activation, long-range inhibition* which is the standard mechanism for a diffusively-driven instability. For example, suppose without loss of generality that u is the activator in equation (1) and v is the inhibitor. Thus $f_u > 0$ and $g_v < 0$. From inequalities (24) and (27) we require

$$0 > \gamma(g_v + f_u) - 2h_* > (d - 1)(h_* - \gamma f_u) + \gamma(d_u f_v + d_v g_u)$$

where $\gamma > 0$.

- (a) In the absence of growth and cross-diffusion, i.e. when $h_* = 0$ and $d_u = d_v = 0$, we immediately have $0 > (1 - d)f_u$ and hence $1 - d$ is negative. Thus, the inhibitor has to diffuse faster than the activator in the absence of growth and cross-diffusion for an instability to be possible.
- (b) In the absence of growth, i.e. $h_* = 0$, but with cross-diffusion in both components we have

$$(1 - d)f_u + (d_u f_v + d_v g_u) < 0.$$

Hence, we can take $0 < d \leq 1$ which implies that

- (i) if $f_v > 0$ and $g_u > 0$, then at least one of the cross-diffusion coefficients must be negative and both must satisfy $d - d_u d_v > 0$, $d_u f_v + d_v g_u < 0$ and $|d_u f_v + d_v g_u| > (1 - d)f_u$,
- (ii) if $f_v < 0$ and $g_u < 0$, then either at least one of the cross-diffusion coefficients must be negative or both are positive, and for both cases, they must satisfy $d - d_u d_v > 0$, $d_u f_v + d_v g_u < 0$ and $|d_u f_v + d_v g_u| > (1 - d)f_u$,
- (iii) if f_v and g_u are of opposite signs, then the choice of the cross-diffusion coefficients are restricted by the inequalities $d - d_u d_v > 0$, $d_u f_v + d_v g_u < 0$ and $|d_u f_v + d_v g_u| > (1 - d)f_u$.
- (c) The presence of growth, i.e. $h_* \neq 0$ does not alter the fact that $0 < d \leq 1$ for the reaction-diffusion system with linear cross-diffusion in both components, and therefore, the above characterisation of the cross-diffusion and reaction-kinetics still holds.

It follows therefore that non-standard reaction-kinetics such as those of the form *short-range inhibition, long-range activation, short-range inhibition, long-range inhibition, short-range activation, long-range activation, same-range inhibitor-inhibitor* (i.e. $d = 1$), *same-range activator-activator* (i.e. $d = 1$), and *same-range activator-inhibitor* (i.e. $d = 1$) can also generate patterns in the presence of cross-diffusion in both components on stationary as well as on evolving domains.

2. *In contrast to the autonomous case* an activator and inhibitor interaction is not required to generate an instability; for example, two activators can satisfy the instability constraints. Again suppose that u is the activator in equation (1) so that $f_u > 0$. Using inequality (24) we find

$$g_v < \left(\frac{2h_*}{\gamma} - f_u \right) < \frac{2h_*}{\gamma},$$

where $\gamma > 0$. Thus, for $h_* = 0$, as with no growth, we have $g_v < 0$, implying that v must be an inhibitor. In contrast for $h_* > 0$ we clearly are not required to have $g_v < 0$ and hence the biochemical corresponding to the concentration v can also be an activator without making a diffusively-driven instability impossible. Therefore an *activator-activator* (on growing domains)

and *inhibitor-inhibitor* (on contracting domains) mechanisms could give rise to Turing patterns only in the presence of domain growth.

4. Exhibiting cross-diffusion induced parameter spaces on evolving domains. To illustrate our theoretical findings, we briefly introduce slow, isotropic growth for exponential, linear and logistic profiles of the domain, calculating functions associated with domain evolution such as $h(t)$ required for the subsequent explorations. Our goal is to compute and exhibit parameter spaces induced by domain evolution for a reaction-diffusion system with cross-diffusion. We will show that cross-diffusion coupled with domain evolution substantially alter classical parameter spaces as well as exhibiting new spaces that emerge only in the presence of domain growth.

Type of growth	Growth Function $\varphi(t)$	$h(t) = \nabla \cdot \mathbf{V}$	$q(t) = e^{-\int_{t_0}^t h(\tau) d\tau}$
Linear	$\varphi(t) = rt + 1$	$h(t) = \frac{m r}{rt+1}$	$q(t) = \left(\frac{1}{rt+1}\right)^m$
Exponential	$\varphi(t) = e^{rt}$	$h(t) = m r$	$q(t) = e^{-mrt}$
Logistic	$\varphi(t) = \frac{\kappa A e^{\kappa r t}}{1 + A e^{\kappa r t}},$ $A = \frac{1}{\kappa - 1}$	$h(t) = m r (\kappa - \varphi(t))$	$q(t) = \left(\frac{e^{-\kappa r t} + A}{1 + A}\right)^m$

TABLE 1. Table illustrating the function $h(t)$ for linear, exponential and logistic growth functions. Note that $q(t)$ is as defined and used in Section 3.2. κ is the carrying capacity (final domain size) corresponding to the logistic growth function.

4.1. Examples: Uniform, isotropic growth. Let us assume that the domain growth is spatially linear and, in higher spatial dimensions, isotropic. Without any loss of generality, let us assume that $t_0 = 0$. Let $\mathbf{x}(t) = \boldsymbol{\xi}\varphi(t)$ where $\varphi(t) > 0$ is the domain growth function satisfying $\varphi(0) = 1$. We can compute the domain (mesh) velocity as

$$\mathbf{a}(\mathbf{x}, t) \stackrel{def}{=} \frac{\partial \mathbf{x}}{\partial t} \Big|_{\boldsymbol{\xi}} = \boldsymbol{\xi} \dot{\varphi}(t) = \frac{\dot{\varphi}(t)}{\varphi(t)} \mathbf{x},$$

and hence it can be easily shown that

$$h(t) := \nabla \cdot \mathbf{V} = m \frac{\dot{\varphi}(t)}{\varphi(t)} \sim O\left(\frac{m\epsilon}{T_{dyn}}\right),$$

where m defines the number of spatial dimensions. In Table 1 we show the corresponding $h(t)$ for linear, exponential and logistic growth functions, with $\kappa \neq 1$. The definition of A in this table ensures that $\varphi(0) = 1$.

Lemma 4.1. *Let us assume that the domain growth is spatially linear and, in higher spatial dimensions, isotropic. Then for linear and logistic domain evolution profiles, the function*

$$h(t) := m \frac{\dot{\varphi}(t)}{\varphi(t)}, \quad m \geq 1,$$

is a monotonically decreasing function whose limit tends to zero, i.e.

$$\lim_{t \rightarrow \infty} h(t) = 0.$$

Proof. The proof follows clearly from the definitions of $h(t)$ shown in Table 1. \square

Corollary 1. For the case of spatially linear, isotropic exponential growth, with growth rate $r > 0$, then

$$h(t) := mr$$

is time-independent [23].

4.2. Activator-depleted model: An illustrative example. For illustrative purposes let us consider the *activator-depleted* substrate model [10, 32, 35] also known as the Brusselator model given by

$$f(u, v) = a - u + u^2 v, \tag{46}$$

$$g(u, v) = b - u^2 v, \tag{47}$$

where a and b are positive parameters to be selected from domain- and cross-diffusion-induced parameter spaces.

4.2.1. Exponential domain evolution. In this section, we exhibit various parameter spaces induced by domain evolution in the presence of linear cross-diffusion. For a fixed value of the growth rate r , the parameter spaces are stationary since conditions (24)-(28) defining the parameter spaces are independent of time t . In all our simulations, except where stated, we take three illustrative examples by fixing $r = 0$ (which is the stationary case), $r = 0.02$ and $r = 0.08$ and then vary the diffusion and cross-diffusion coefficients as outlined by the following cases.

Cross-diffusion driven instability on evolving domains for $d > 1$. Fix $d = 10$ and vary the cross-diffusion coefficients as follows:

1. $d_u = 0$ and $d_v = 1$, i.e. cross-diffusion in the u -equation only (blue).
2. $d_u = 1$ and $d_v = 1$, i.e. cross-diffusion in the u and v equations (green).
3. $d_u = 0$ and $d_v = 0$, i.e. no cross-diffusion (red).
4. $d_u = 1$ and $d_v = 0$, i.e. cross-diffusion in the v -equation only (light blue).

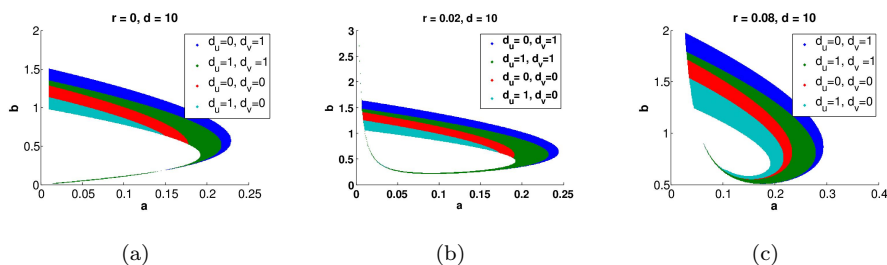


FIGURE 1. Parameter spaces for different exponential growth rates with diffusion coefficient $d = 10$ and cross-diffusion coefficients varied accordingly. (a) In the absence of growth, and (b)-(c): in the presence of growth: exponential growth with rates $r = 0.02$ (b) and $r = 0.08$ (c).

For a fixed set of diffusion and cross-diffusion coefficients, varying the exponential growth rate r results in larger and larger parameter spaces emerging during the exponential evolution of the domain. On the other hand, fixing the exponential growth rate r , parameter spaces of different sizes are obtained with the largest parameter space corresponding to the reaction-diffusion system with cross-diffusion in the u -equation only, while the smallest parameter space corresponds to the reaction-diffusion system with cross-diffusion in the v -equation only. This is consistent with theoretical results presented in [26] for the case of stationary domains.

Cross-diffusion driven instability on evolving domains for $d = 1$ and $d_u = 1$. Here we fix $d = 1$ and $d_u = 1$ and vary positively only the cross-diffusion coefficient d_v such that the inequality $d - d_u d_v > 0$ is satisfied. Figure 2 shows the cross-diffusion parameter spaces with cross-diffusion coefficient $d_v = 0.5$ (light blue), $d_v = 0.6$ (red), $d_v = 0.7$ (green) and $d_v = 0.8$ (dark blue), for different exponential growth rates.

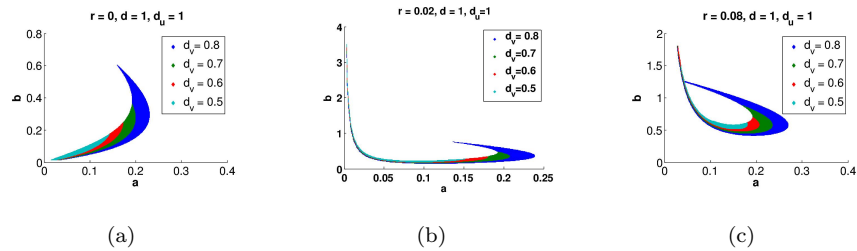


FIGURE 2. Parameter spaces for an exponential evolution of the domain with diffusion coefficient $d = 1$ and cross-diffusion coefficient $d_u = 1$. The cross-diffusion coefficient d_v is varied accordingly. (a) In the absence of growth, and (b)-(c): in the presence of growth: exponential growth with rates $r = 0.02$ (b) and $r = 0.08$ (c).

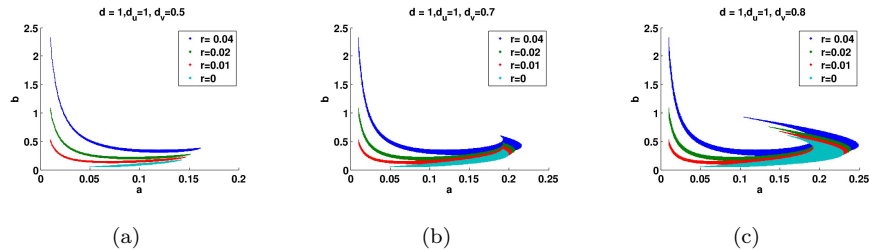


FIGURE 3. Superimposition of the individual parameter spaces shown in Figure 2 with diffusion coefficient $d = 1$ and cross-diffusion coefficient $d_u = 1$ for different exponential growth rates: $r = 0$ (light blue), $r = 0.01$ (red), $r = 0.02$ (green) and $r = 0.04$ (blue). The cross-diffusion coefficient d_v is varied accordingly.

As $d_v \rightarrow 1$, we observe larger and larger parameter spaces, while when $d_v \rightarrow 0$, smaller and smaller parameter spaces are exhibited and these vanish as d approaches zero (see Figure 3). In Figure 3 we superimpose parameter spaces when (i) d_v is varied positively and (ii) the exponential growth rate r is also varied. We observe that for lower values of d_v , distinct parameter spaces are obtained, while for larger values of d_v approaching one, the parameter spaces overlap substantially.

Cross-diffusion driven instability on evolving domains for $d = 1$ and $d_v = 1$. Here we fix $d = 1$ and $d_v = 1$ and vary positively only the cross-diffusion coefficient d_u . Figure 4 shows the cross-diffusion parameter spaces with cross-diffusion coefficient $d_u = 0.5$ (light blue), $d_u = 0.6$ (red), $d_u = 0.7$ (green) and $d_u = 0.8$ (dark blue), for different exponential growth rates.

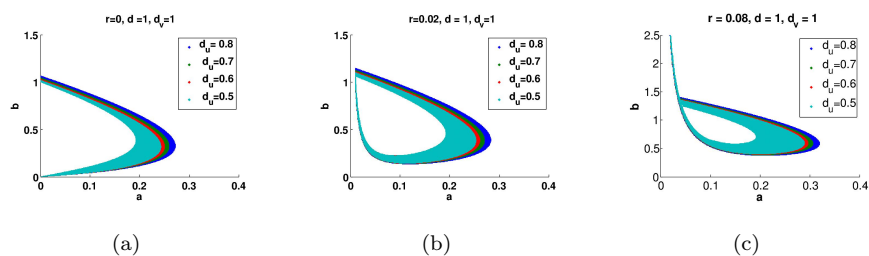


FIGURE 4. Parameter spaces for an exponential evolution of the domain with diffusion coefficient $d = 1$ and cross-diffusion coefficient $d_v = 1$. The cross-diffusion coefficient d_u is varied positively. (a) In the absence of growth, and (b)-(c): in the presence of growth: exponential growth with rates $r = 0.02$ (b) and $r = 0.08$ (c).

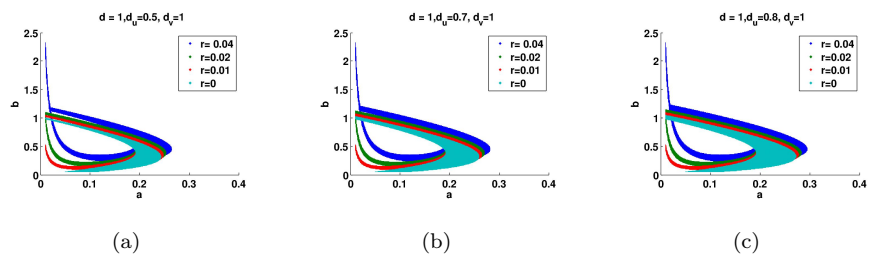


FIGURE 5. Superimposition of the individual parameter spaces shown in Figure 4 with diffusion coefficient $d = 1$ and cross-diffusion coefficient $d_v = 1$ for different exponential growth rates: $r = 0$ (light blue), $r = 0.01$ (red), $r = 0.02$ (green) and $r = 0.04$ (blue). The cross-diffusion coefficient d_u is varied positively.

Similarly, variations in d_u results in smaller and smaller parameter spaces as $d_u \rightarrow 0$ and larger and larger parameter spaces as $d_u \rightarrow 1$. Individual parameter spaces are superimposed as illustrated in Figure 5. As the exponential growth rate

r increases, for a fixed set of diffusion and cross-diffusion coefficients, substantially different parameter spaces emerge. Exponential evolution of the domain results in substantially topologically different parameter spaces from those obtained in the absence of growth.

Negative cross-diffusion driven instability on evolving domains for $d = 1$ and $d_v = 1$. Unlike previous examples, we fix $d = 1$ and $d_v = 1$ and vary negatively only the cross-diffusion coefficient d_u such that the inequality $d - d_u d_v > 0$ is satisfied. Figure 6 shows the cross-diffusion parameter spaces with cross-diffusion coefficient $d_u = -0.8$ (light blue), $d_u = -0.7$ (red), $d_u = -0.6$ (green) and $d_u = -0.5$ (dark blue), for different exponential growth rates.

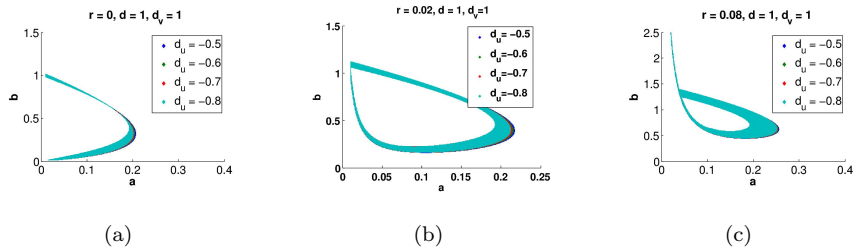


FIGURE 6. Parameter spaces for an exponential evolution of the domain with diffusion coefficient $d = 1$ and $d_v = 1$. The cross-diffusion coefficient d_u is varied negatively. (a) In the absence of growth, and (b)-(c): in the presence of growth: exponential growth with rates $r = 0.02$ (b) and $r = 0.08$ (c).

We observe that substantially and topologically different parameter spaces are obtained as the exponential growth rate is varied. However, for a fixed exponential growth rate, variations in the cross-diffusion coefficient do not alter substantially the parameter spaces. This is unlike previous results where variations in cross-diffusion coefficients could alter substantially the parameter spaces (see Figures 1-2, for example).

Short-range inhibition, long-range activation: Cross-diffusion induced parameter spaces. For the first time, we present a *short-range inhibition, long-range activation* model that can only give rise to pattern formation in the presence of cross-diffusion. From the cross-diffusion driven instability condition $d - d_u d_v > 0$, we take $0 < d = 0.5 < 1$, i.e. $0 < D_v < D_u$ in dimensional units, and therefore the activator u diffuses much faster than the inhibitor v . To proceed, we further fix $d_v = 0.8$ and vary negatively d_u such that the condition $d - d_u d_v > 0$ is satisfied. Figure 7 shows the parameter spaces demonstrating the ability of the model system to generate patterns in the presence of cross-diffusion. Without cross-diffusion, such spaces do not exist. We note that d_u is constrained by the fact that $-1 < d_u < 0$ in order for the u -equation in system (1) to be well posed. On the other, d_v is constrained by the cross-diffusion driven instability condition (26). As the cross-diffusion coefficients d_u and d_v increase and decrease towards zero values, cross-diffusion driven instability spaces reduce in size and disappear altogether (results not shown). This is consistent with theoretical result that for diffusion-driven instability to occur for

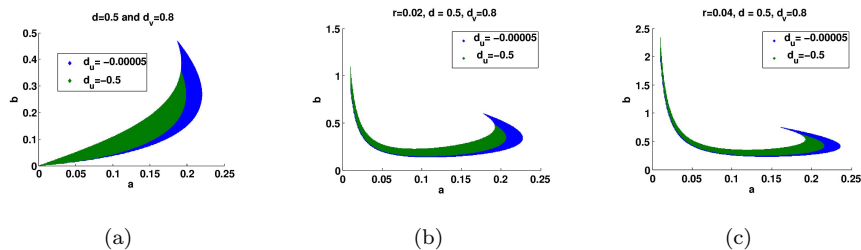


FIGURE 7. Parameter spaces for a *short-range inhibition, long-range activation* with diffusion coefficient $d = 0.5$ and cross-diffusion coefficient $d_v = 0.8$. We vary d_u negatively. (a) In the absence of growth, and (b)-(c): in the presence of growth: exponential growth with rates $r = 0.02$ (b) and $r = 0.04$ (c).

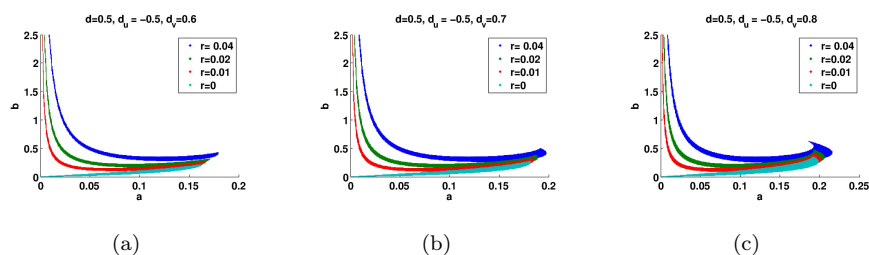


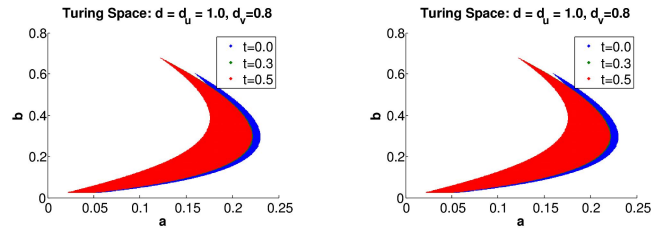
FIGURE 8. Plots of superimposed parameter spaces for different exponential growth rates r with fixed diffusion coefficient $d = 0.5$, and cross-diffusion coefficient $= d_u = -0.5$. We vary the cross-diffusion coefficient d_v as follows: (a) $d_v = 0.5$, (b) $d_v = 0.7$ and (c) $d_v = 0.8$.

classical reaction-diffusion systems the diffusion coefficient d must be different from one.

In Figure 8 we exhibit superposition of parameter spaces as we vary (i) the cross-diffusion coefficient d_v positively and (ii) the exponential growth rate r . Here we have fixed the diffusion coefficient $d = 0.5$ and the cross-diffusion coefficient $d_u = -0.5$. For small values of d_v , distinct parameter spaces are obtained, while for large values of d_v , overlapping parameter spaces are exhibited. Interestingly, substantially large parameter spaces are obtained during growth development compared to those obtained in the absence of domain growth. It is therefore clear, that domain growth enhances the formation of pattern formation.

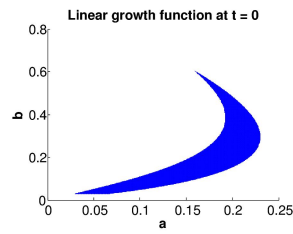
4.2.2. *Linear and logistic domain evolution.* Next we compute parameter spaces generated by linear and logistic growth functions for two-dimensional evolving domains. For the linear and logistic growth functions we compute the time-dependent solutions $(u_S(t), v_S(t))$ which satisfy the differential equations

$$\frac{du_S}{dt} = \gamma a - (\gamma + h(t))u_S + \gamma u_S^2 v_S, \tag{48}$$

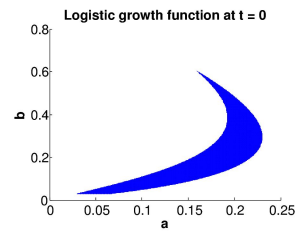


(a) Linear growth functions

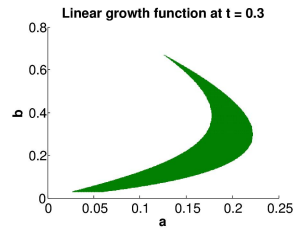
(b) Logistic growth functions



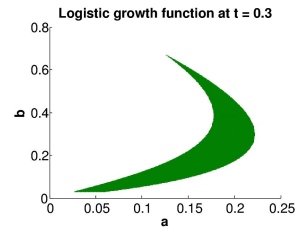
(c)



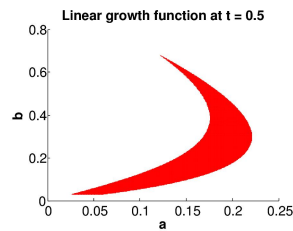
(d)



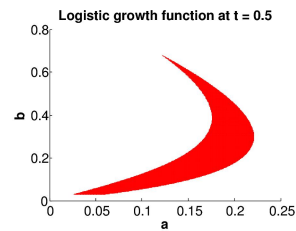
(e)



(f)



(g)



(h)

FIGURE 9. Cross-diffusion induced parameter spaces for linear (left column) and logistic (right column) growth functions computed at time $t = 0, 0.3$ and 0.5 . The individual spaces for each growth function are shown in (c) - (h).

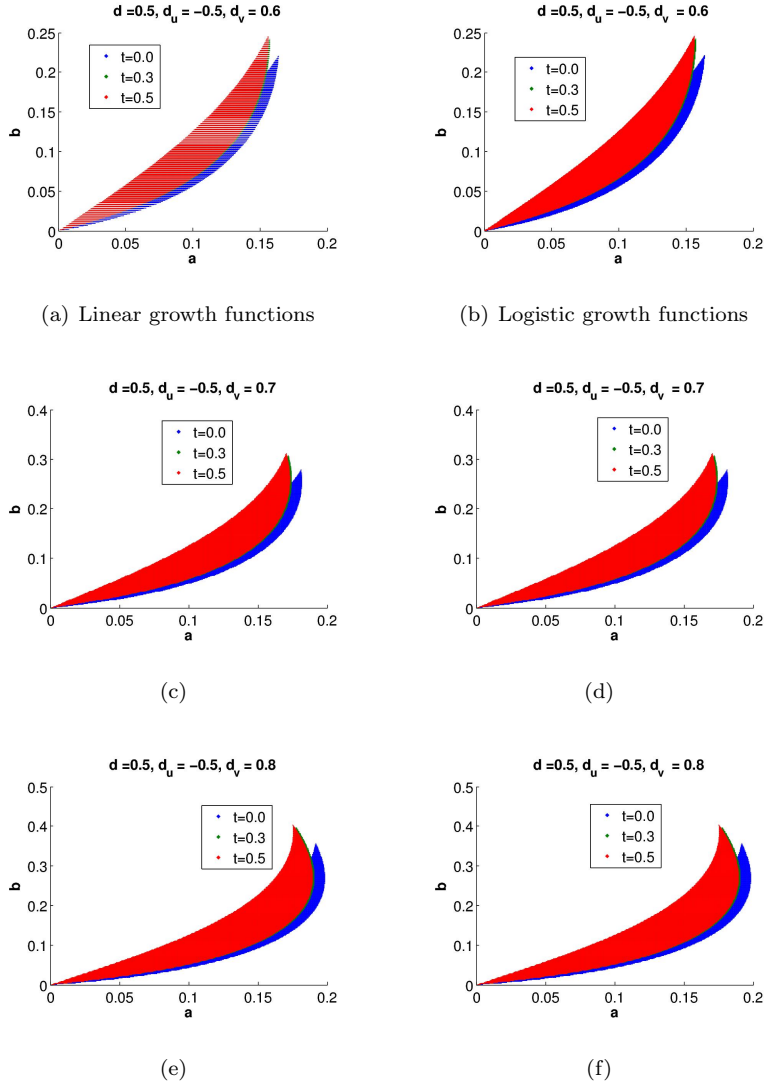


FIGURE 10. Cross-diffusion induced parameter spaces for linear (left column) and logistic (right column) growth functions computed at time $t = 0, 0.3$ and 0.5 . The cross-diffusion parameter value d_v is varied as illustrated.

$$\frac{dv_S}{dt} = \gamma b - h(t) v_S - \gamma u_S^2 v_S, \tag{49}$$

where $h(t) = \nabla \cdot \mathbf{V}$ and given initial values at time $t_0 = 0$. From the linear growth function, $h(t) = \frac{m r}{r t + 1}$ and similarly for the logistic growth function, $h(t) = m r (\kappa - \varphi(t))$ where $\varphi(t) = \frac{A \kappa e^{\kappa r t}}{1 + A e^{\kappa r t}}$, with $A = \frac{1}{\kappa - 1}$. Let us take $r = 0.01 (\ll 1)$, $m = 2.0$, $\kappa = 2$ and $A = 1$. In all our numerical examples, initial conditions $(u_S(0), v_S(0))$ are taken as small random perturbations around the uniform steady

state $\left(a + b, \frac{b}{(a+b)^2}\right)$ obtained on stationary domains. The cross-diffusion and domain growth induced parameter spaces in this section are independent of these random initial conditions.

In order to compute the parameter spaces given by conditions (24)-(28) for the cases of linear and logistic growth functions, the non-autonomous differential equations (48)-(49) must be solved for every point (a, b) in the plane at any given time t thereby giving rise to time-dependent parameter spaces.

Figure 9-10 exhibit time-dependent parameter spaces generated as a result of linear (first column) and logistic (second column) growth functions of the domain. The first column of Figure 9 corresponds to the linear growth; (c), (e) and (g) are the individual spaces of (a) and the second column corresponds to the logistic growth; (d), (f) and (h) are individual spaces of (b).

Unlike parameter spaces generated by the exponential growth, linear and logistic growth functions generate parameter spaces which overlap substantially. Linear and logistic growth functions generate larger but topologically similar parameter spaces to those obtained in the absence of domain growth. This is in contrast to the exponential growth which generates larger and sometimes topologically different parameter spaces.

In Figure 10 we present parameter spaces corresponding to the linear and logistic growth functions when we fix $d = 0.5$, $d_u = -0.5$ and vary $d_v = 0.6, 0.7, 0.8$ respectively. As $d_v \rightarrow 1$, larger and larger parameter spaces are observed, while $d_v \rightarrow 0$, smaller and smaller parameter spaces emerge.

Remark 6. It must be noted that all the parameter spaces exhibited in Figures 2-10 are cross-diffusion and domain-growth induced spaces, such parameter spaces do not exist for the classical autonomous system of reaction-diffusion equations.

5. Domain- and cross-diffusion induced patterns on evolving domains.

In this section we exhibit domain- and cross-diffusion induced patterns on planar evolving square domains. Surface- and cross-diffusion induced patterns on evolving surfaces are presented in Madzvamuse and Barreira [25]. Unlike any previous studies of these types of models, our focus is to present patterns generated from a non-standard reaction-diffusion system of the form *long-range activation, short-range inhibition* model that will only give rise to patterning in the presence of cross-diffusion. The effects of domain growth enhances patterning independent of the initial conditions. The patterns exhibited in this section can only be obtained in the presence of cross-diffusion, such a model of the form *long-range activation, short-range inhibition* does not give rise to patterning in the absence of cross-diffusion, with or without domain evolution. For illustrative purposes, we take an *activator-depleted* model known to satisfy the cross/pure kinetics conditions [10, 32, 35]. Our focus is to study the effects of cross-diffusion on a standard reaction-diffusion model in the presence of domain evolution. We leave studies of non-standard reaction kinetics capable of giving rise to patterning only in the presence of cross-diffusion and domain evolution for future studies. To the best of the authors' knowledge, only models of the form *long-range inhibition; short-range activation* have the ability to give rise to patterning in the absence of cross-diffusion. We will depart from this framework and select diffusion and cross-diffusion parameter values such that a *short-range inhibition; long-range activation* can exhibit cross-diffusion induced patterns on evolving domains. In Madzvamuse and Barreira [25] we presented a wide range of patterns on evolving domains and surfaces. In most of these examples,

parameter values were selected outside the standard Turing parameter space (see [25] for details). Comparisons were then made between patterns obtained between the autonomous standard reaction-diffusion model and the non-autonomous non-standard reaction-diffusion model.

We select two sets of model kinetic parameter values from parameter spaces induced by exponential, linear and logistic growth functions as illustrated in Figures 7 (a) and 10, respectively. These are (i) $a = 0.15$, $b = 0.2$ and (ii) $a = 0.15$ and $b = 0.15$ respectively. The diffusion and cross-diffusion coefficients are fixed as $d_v = 0.5$, $d_u = -0.5$ and $d_{uv} = 0.6$ (corresponding to case (i)) and $d_{uv} = 0.8$ (corresponding to case (ii)) above respectively. For all the growth functions, we take the growth rate $r = 0.01$. For illustrative purposes, we take $\gamma = 200$. In all the cases, random initial perturbations around the uniform steady state which is calculated on stationary domains are prescribed.

Numerical simulations are carried out using the evolving or moving finite element method; details of the numerical method are given in Madzvamuse *et al.*, [25]. The moving grid finite element method has been applied extensively to study reaction-diffusion systems on stationary and evolving domains with applications to developmental biology. The reader is referred to [4, 15, 18, 19, 20, 21, 25, 26] for further references detailing the numerical method and its applications. In Figures 11 - 22 we exhibit the results of our simulations, validating theoretical results presented in the previous section. Furthermore, in order to understand the evolution of the bifurcation process during growth development, we plot the evolution of the log of the L_2 -norm of the errors between successive numerical iterate solutions corresponding to patterns shown in Figures 12, 14, 16, 18, 20 and 22.

Figure 11 shows pattern formation during growth development for the parameter values $d = 0.5$, $a = 0.15$, $b = 0.2$, $d_u = -0.5$, $d_v = 0.6$ and $\gamma = 200$. We observe the formation of spots which correlate to the growth of the error norm at the initial stages of growth (see first peak observed in Figure 12); these are rapidly destabilised; with stripe patterns forming (which also now correlate to the second sharp pick observed in Figure 12). The stripe patterns are stable to domain growth for a substantial amount of time (this is manifested by the reduction in the errors which become almost constant as illustrated in Figure 12). Destabilisation of the stripes results in the rapid formation of spot patterns (of different wavelenghts) but these are less stable to domain growth (compare Figure 11 (f) and (g)), thereby giving way to the formation of stripe patterns again. This is reflected in the error graph where there is a rapid growth and decay in errors, but once the spots are formed, there is a rapid, almost period growth and decay in errors. This evolutionary process of spots forming and being destabilised rapidly and then the formation of stripes or spots continues almost periodically. We observe the formation of “peanut” patterns, reminiscent of the *activator-depleted* model.

The evolutionary process becomes substantially different if a different growth function is employed. For example, a linear evolution of the domain results in the formation of spot patterns, similar to the exponential growth at the very early stages of growth development, and these transient into stripes, which are stable for a substantially longer period of time than for the case of the exponential growth (compare Figures 12 and 14). In fact, for the linear growth, the only patterns to form later during growth development are spots which are only stable for a vey short time; these give way to the formation of stripe patterns which continue to be stable (for as long as we evolved the domain).

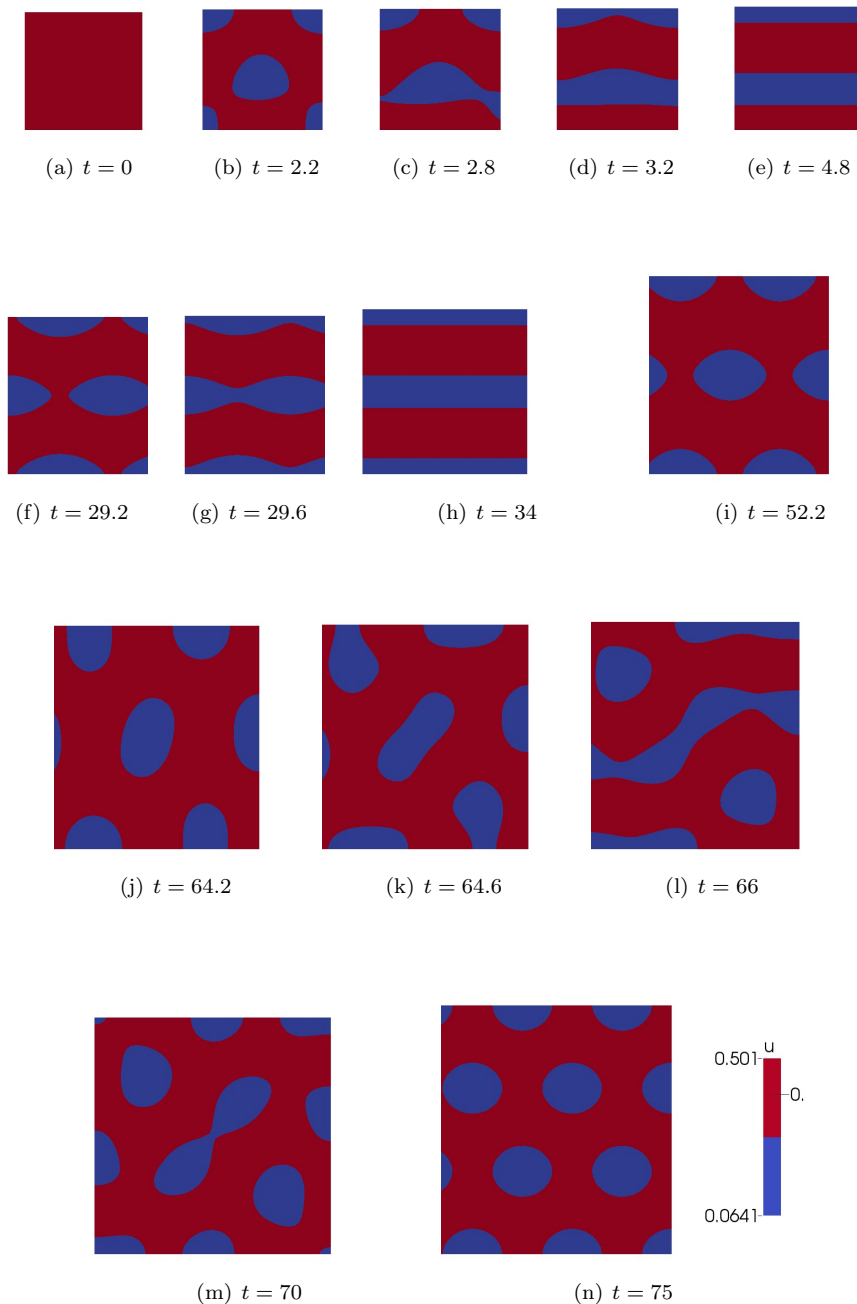
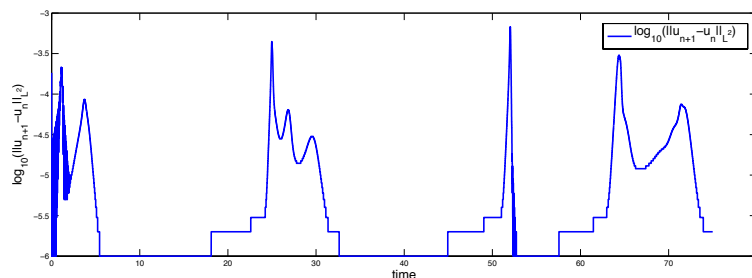


FIGURE 11. Numerical simulations corresponding to the chemical specie u with parameters $d = 0.5$, $a = 0.15$, $b = 0.2$, $d_u = -0.5$, $d_v = 0.6$ and $\gamma = 200$. Domain evolving of the unit square according to the exponential growth function with growth rate $r = 0.01$.



(a) $t = 0$

FIGURE 12. Plot of the evolution of the log of the L_2 -norm of the errors between successive numerical iterate solutions corresponding to patterns shown in Figure 11, for the case of exponential growth.

On the other hand, employing a logistic growth function, we observe a remarkably different bifurcation process during domain evolution. The error graph shows only three substantial bifurcation processes (compared to six for the exponential and four or five for the linear growth functions). The logistic growth function is characterised by rapid growth at the early stages (which might imply that lower modes are almost unexcitable during growth development), followed by a linear growth at mid-stages of the domain evolution and then saturation of the growth evolution at later stages. The three phases of logistic growth are therefore characterised by stripes bifurcating into spot-stripe patterns which subsequently transient into circular patterns (assuming one is following the red patterns), and these finally bifurcate into stripes which remain stable as the domain approaches the final size (see Figure 15 and 16).

By selecting a different set of parameter values, for example, $d = 0.5$, $a = 0.15$, $b = 0.15$, $d_u = -0.5$, $d_v = 0.8$ and $\gamma = 200$, substantially different bifurcation processes and sequences are observed for the exponential, linear and logistic growth functions. Small variations in the model parameter values result in substantially different patterning processes as illustrated in Figures 17, 19 and 21. The characteristics of the evolution of the bifurcation processes remain almost similar to those shown in Figures 12, 14 and 16 (compare to Figures 18, 20 and 22, respectively). The exponential growth profile is characterised by continuous evolution of transient patterns, with less and less periods of constant stability of solutions during growth development. The opposite holds true for the linear and logistic growth functions, the periods of constant stability increase with further domain growth (see Figures 20 and 22). For this set of parameter values, we observe some very interesting patterns forming, for example, spots and stripes are formed simultaneously (see Figures 17 (m), 19 (f), 21 (f), respectively). To the authors' best knowledge, these patterns are the first to be exhibited and are solely due to cross-diffusion. We also observe, as before, that linear and logistic growth functions seem to stabilise more robustly stripe patterns at later stages of the domain evolution than spot patterns. The exponential evolution favours the continuous formation of stripe, spot, stripe-spot and circular patterns as the domain continues to evolve.

Remark 7. All the numerical results presented in this section correspond to the model system (1) with model parameter values selected such that the system is of the

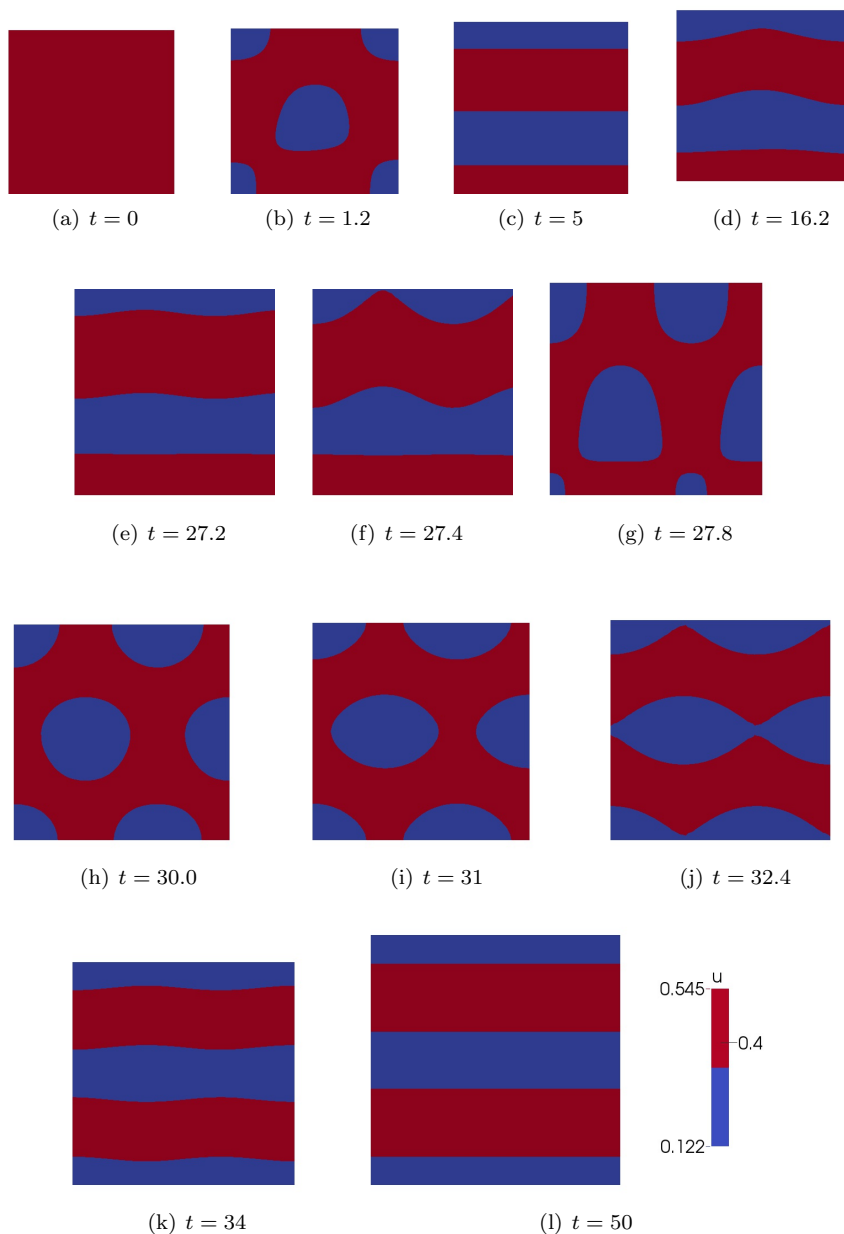


FIGURE 13. Numerical simulations corresponding to the chemical specie u with parameters $d = 0.5$, $a = 0.15$, $b = 0.2$, $d_u = -0.5$, $d_v = 0.6$ and $\gamma = 200$. Domain evolving of the unit square according to the linear growth function with $r = 0.01$.

form *long-range activation short-range inhibition* model. Such a model does not give rise to Turing diffusion-driven instability in the absence of cross-diffusion nor domain growth. As a result, such patterns can not be observed on stationary domains in the absence of cross-diffusion. For detailed comparisons between patterns obtained

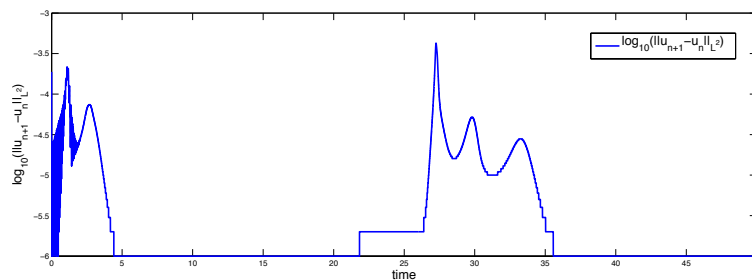
(a) $t = 0$

FIGURE 14. Plot of the evolution of the log of the L_2 -norm of the errors between successive numerical iterate solutions corresponding to patterns shown in Figure 13, for the case of linear growth.

from model system (1) and that without cross-diffusion nor domain growth, the interested reader is referred to Madzvamuse and Barreira [25].

6. Conclusion and discussion. In this article we have generalised substantially the theory for reaction-diffusion systems with cross-diffusion to consider the effects of domain evolution on cross-diffusion induced patterning. Our results reveal that in the presence of cross-diffusion and domain evolution, the restrictive conditions associated with *long range inhibition, short range activation* can be relaxed to allow a wide range of model parameter values and reaction-kinetics that would otherwise not give rise to patterning either in the absence of cross-diffusion and/or domain evolution. We have shown that a *long range activation, short range inhibition* can generate patterns only in the presence of domain evolution and/or cross-diffusion. These theoretical findings open new research directions, both experimentally and theoretically, where non-standard mechanisms for patterning can be considered and designed.

Theoretically, we have derived and proved the conditions for cross-diffusion driven instability. By using these conditions, we then computed and exhibited a wide variety of parameter spaces for exponential, linear and logistic growth functions. Our results unravel the emergence of parameter spaces with interesting characteristics. For a fixed set of appropriate parameter values, exponential evolution of the domain results in substantially different spaces from those obtained in the absence of domain evolution. Although linear and logistic growth functions yield larger parameter spaces in the presence of domain evolution, these are topologically similar to those obtained in the absence of domain evolution [19, 24, 25].

Our analytical results reveal that unlike the restrictive diffusion-driven instability conditions on stationary domains, in the presence of cross-diffusion coupled with domain evolution, it is no longer necessary to enforce cross nor pure kinetic conditions. The restriction to *activator-inhibitor* kinetics to induce pattern formation on a growing biological system is no longer a requirement. Reaction-cross-diffusion models with equal diffusion coefficients in the principal components as well as those of the *short-range inhibition, long-range activation* and *activator-activator* form can generate patterns only in the presence of cross-diffusion coupled with domain evolution.

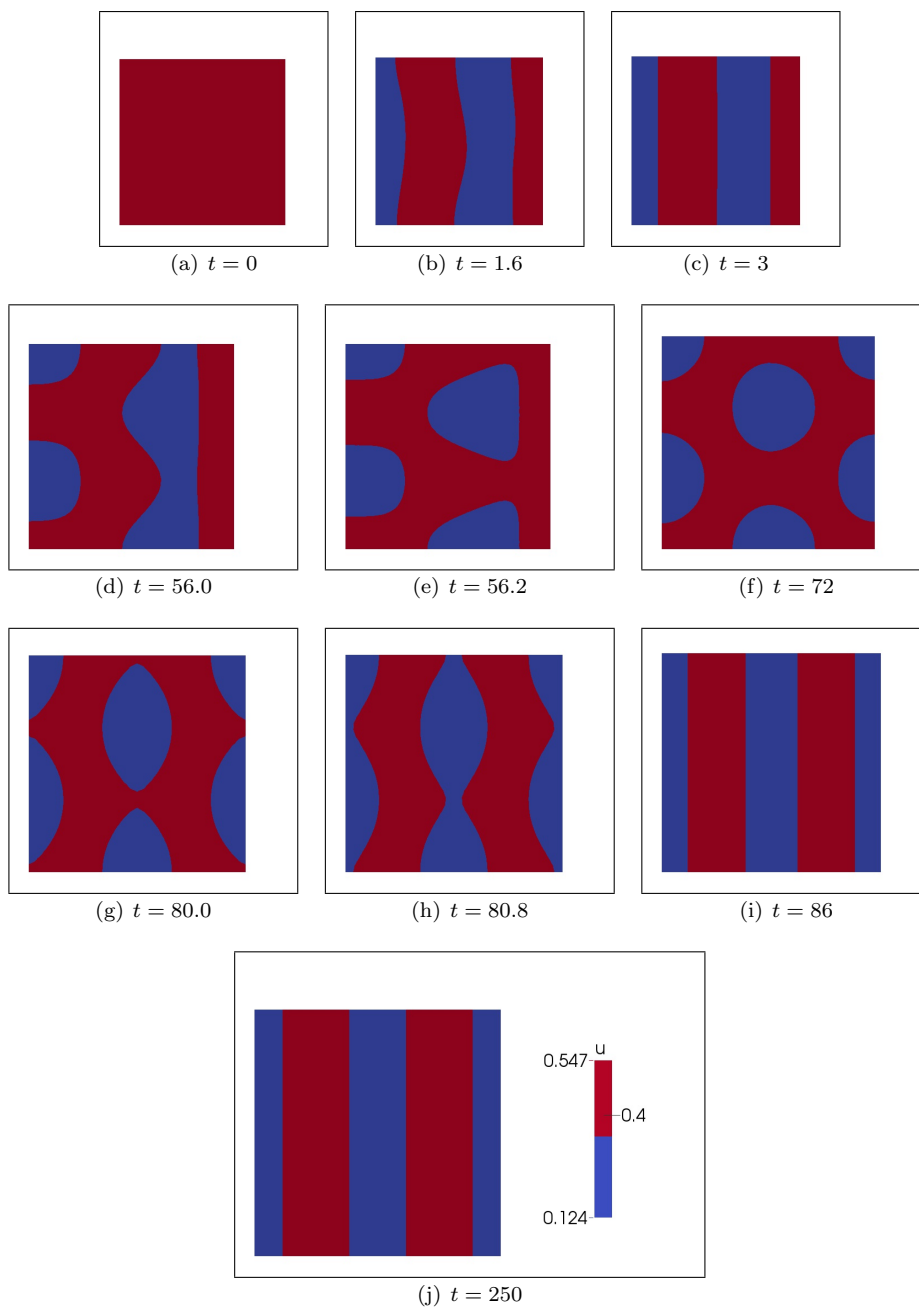
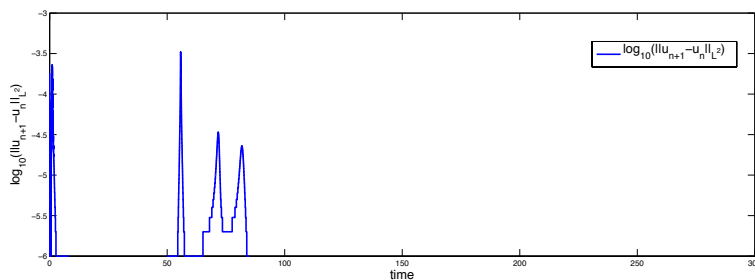


FIGURE 15. Numerical simulations corresponding to the chemical specie u with parameters $d = 0.5$, $a = 0.15$, $b = 0.2$, $d_u = -0.5$, $d_v = 0.6$ and $\gamma = 200$. Domain evolving of the unit square according to the logistic growth function with $r = 0.01$.



(a) $t = 0$

FIGURE 16. Plot of the evolution of the log of the L_2 -norm of the errors between successive numerical iterate solutions corresponding to patterns shown in Figure 15, for the case of logistic growth.

In summary, the following characteristics are exhibited by reaction-diffusion systems with linear cross-diffusion in the presence of an exponential domain growth:

1. Large parameter spaces emerge during an exponential evolution of the domain. In all our simulations, the reaction-diffusion system with cross-diffusion in the u -equation only possesses the largest parameter space in the presence of domain evolution. This is an inherent property of the model and holds true in the absence of domain evolution.
2. On the other hand, the reaction-diffusion system with cross-diffusion in the v -equation only possesses the smallest parameter space during domain evolution, in complete agreement with the model system on stationary domains. Again, this is an inherent property of the model system.
3. In all our simulations, the parameter spaces corresponding to the reaction-diffusion system with cross-diffusion in the v -equation only are sub-spaces (for slow domain evolution) of the parameter spaces corresponding to the reaction-diffusion system without cross-diffusion. These, in turn, are sub-spaces of the reaction-diffusion system with cross-diffusion in both the u and v -equations. Similarly, there parameter spaces are contained fully in the largest parameter spaces corresponding to the reaction-diffusion system with cross-diffusion in the u -equation only. However, for the case of fast domain evolution, distinct and substantially different parameter spaces are obtained.
4. For a given set of diffusion and cross-diffusion values, exponential evolution of the domain results in larger and distinct parameter spaces with or without intersections. The fact that in general there is no overlap between the zero-growth rate parameter spaces and those on evolving domains leads us to conclude that, in general, cross-diffusion driven instability in the absence of growth need not imply diffusively-driven instability in the presence of growth.

To demonstrate the effects of domain evolution on cross-diffusion induced patterning, numerical experiments computed using the evolving or moving finite element method [19, 25] are presented for specific choices of parameter values selected from the cross-diffusion induced parameter spaces. An important key observation is that unlike on stationary domains, pattern evolution during growth development is independent of the initial conditions. On stationary domains, patterns are known to depend crucially on the initial conditions which act as a basin of attraction.

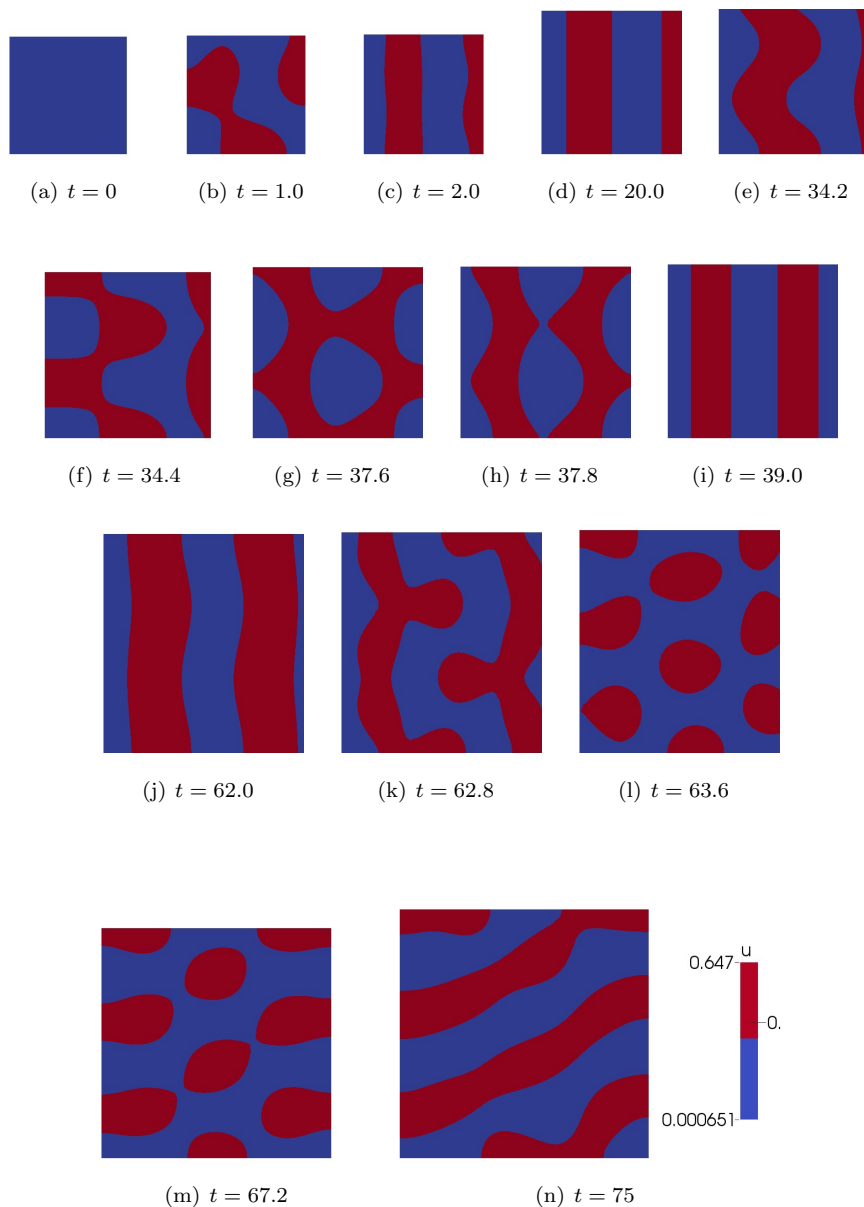


FIGURE 17. Numerical simulations corresponding to the chemical specie u with parameters $d = 0.5$, $a = 0.15$, $b = 0.15$, $d_u = -0.5$, $d_v = 0.8$ and $\gamma = 200$. Domain evolving of the unit square according to the exponential growth function with $r = 0.01$.

Furthermore, domain evolution stabilises patterning which would otherwise be unstable in the absence of domain growth. For example, patterns formed on the final evolving domain are substantially different from those obtained if one computes the model system starting with random initial conditions by taking the final domain stationary (results not shown).

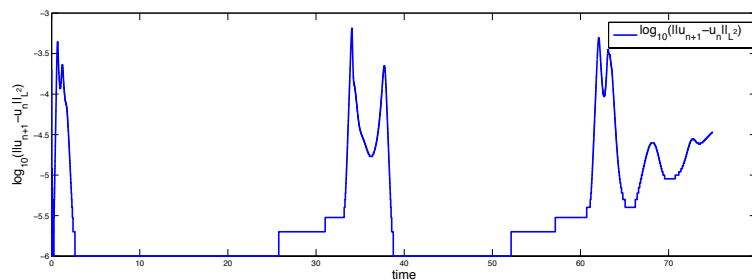
(a) $t = 0$

FIGURE 18. Plot of the evolution of the log of the L_2 -norm of the errors between successive numerical iterate solutions corresponding to patterns shown in Figure 17, for the case of exponential growth.

We have previously reported in the literature that domain growth enhances robustness of certain patterns in a Turing mechanism [27, 31]. In this paper, we have shown that growth does not only induce instability in a reaction-diffusion system with cross-diffusion but that cross-diffusion coupled with domain growth expands substantially the range of mechanisms that can give rise to spatial patterns away from the classical *short-range activation, long-range inhibition* paradigm. Understanding the effects of cross-diffusion to the theory of pattern formation during growth development is crucial in many areas of research such as nanoparticles, surfactants and polymers.

From a theoretical point of view, our studies raise two key research questions to be addressed; namely (i) the derivation of non-standard reaction kinetics that will give rise to cross-diffusion driven-instability only in the presence of cross-diffusion and/or domain evolution and (ii) the derivation of an analytical framework to study bifurcation sequences and processes for non-autonomous reaction-diffusion systems with linear and nonlinear cross-diffusion. It is clear from the L_2 norm graphs of the errors that there exists smooth as well as sharp bifurcation transitions as the transient solutions gain or loose stability during domain evolution. Some of these transitions are reflective of the bifurcation process known as *hysteresis* [30]; only detailed analytical studies of these models on evolving domains will answer and confirm such observations.

Acknowledgments. This work (AM) is supported by the following grants: the Engineering and Physical Sciences Research Council (EP/J016780/1) on *Modelling, analysis and simulation of spatial patterning on evolving biological surfaces* and the Leverhulme Trust research project grant (RPG-2014-149) on *Unravelling new mathematics for 3D cell migration*. This project (AM) has received funding from the European Unions Horizon 2020 research and innovation programme under the Marie Skłodowska-Curie grant agreement No 642866. RB is a Visiting Fellow supported by the EPSRC grant (EP/J016780/1) to collaborate with AM. RB used the computational resources of the Center for Mathematics and Fundamental Applications of the University of Lisbon. The final writing up of this article was undertaken when AM and RB were programme participants of the Isaac Newton Institute for Mathematical Sciences 6-months programme on *Coupling geometric PDEs with physics*

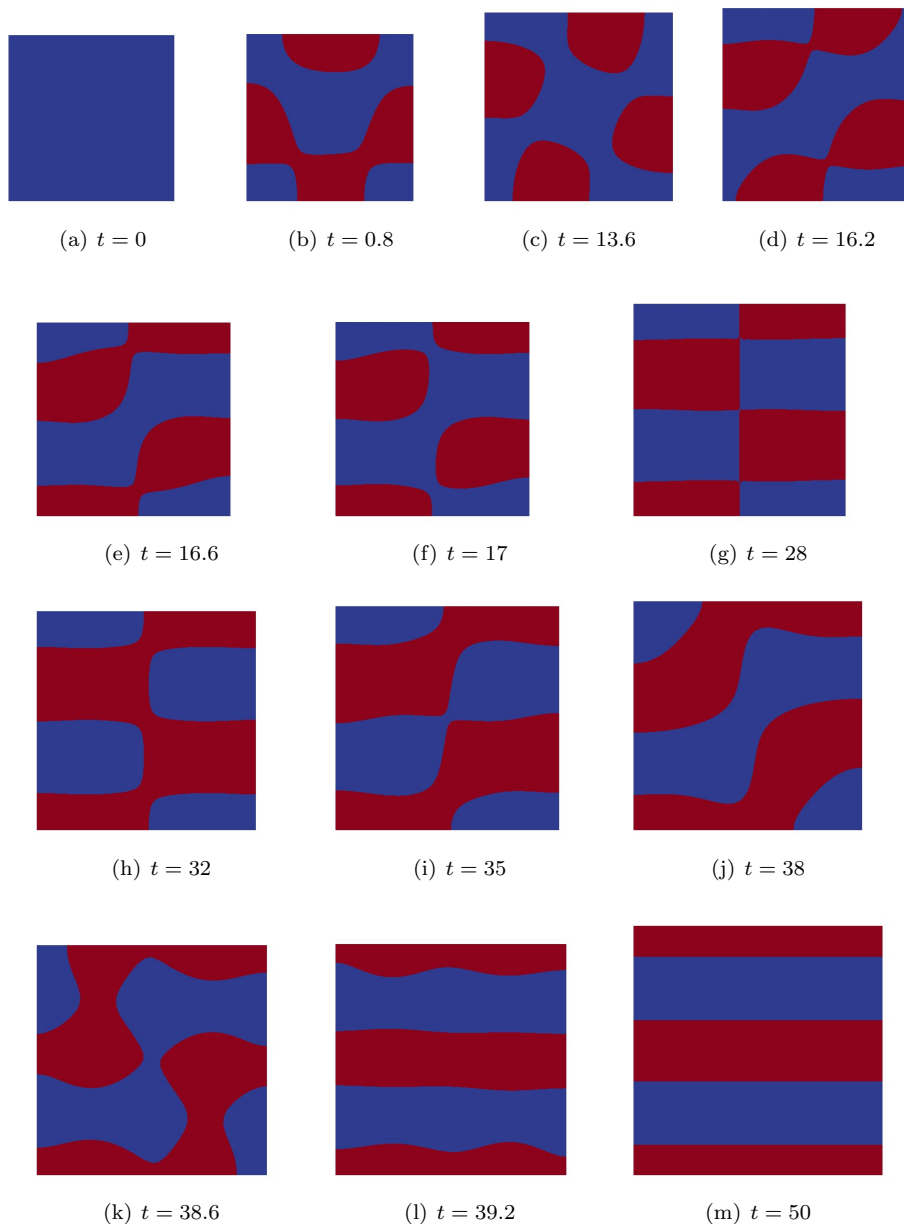


FIGURE 19. Numerical simulations corresponding to the chemical specie u with parameters $d = 0.5$, $a = 0.15$, $b = 0.15$, $d_u = -0.5$, $d_v = 0.8$ and $\gamma = 200$. Domain evolving of the unit square according to the linear growth function with $r = 0.01$.

for cell morphology, motility and pattern formation (13 July - 18 December 2015). This work (AM) was partially supported by a grant from the Simons Foundation.

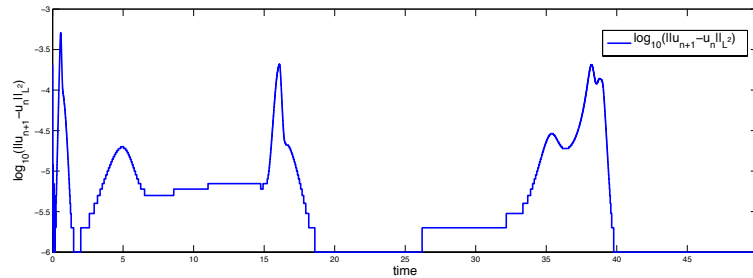
(a) $t = 0$

FIGURE 20. Plot of the evolution of the log of the L_2 -norm of the errors between successive numerical iterate solutions corresponding to patterns shown in Figure 19, for the case of linear growth.

REFERENCES

- [1] D. Acheson, *Elementary Fluid Dynamics*, Oxford University Press, New York, 1990.
- [2] M. Baines, *Moving Finite Elements*, Oxford University Press, New York, 1994.
- [3] J. Bard and I. Lauder, [How well does Turing's Theory of morphogenesis work?](#), *J. Theor. Biol.*, **45** (1974), 501–531.
- [4] R. Barreira, C. M. Elliott and A. Madzvamuse, [The surface finite element method for pattern formation on evolving biological surfaces](#), *J. Math. Biol.*, **63** (2011), 1095–1119.
- [5] V. Capasso and D. Liddo, [Asymptotic behaviour of reaction-diffusion systems in population and epidemic models. The role of cross-diffusion](#), *J. Math. Biol.*, **32** (1994), 453–463.
- [6] V. Capasso and D. Liddo, [Global attractivity for reaction-diffusion systems. The case of nondiagonal diffusion matrices](#), *J. Math. Anal. and App.*, **177** (1993), 510–529.
- [7] E. J. Crampin, W. W. Hackborn and P. K. Maini, [Pattern formation in reaction-diffusion models with nonuniform domain growth](#), *Bull. Math. Biol.*, **64** (2002), 747–769.
- [8] G. Gambino, M. C. Lombardo and M. Sammartino, [Turing instability and traveling fronts for nonlinear reaction-diffusion system with cross-diffusion](#), *Maths. Comp. in Sim.*, **82** (2012), 1112–1132.
- [9] G. Gambino, M. C. Lombardo and M. Sammartino, [Pattern formation driven by cross-diffusion in 2-D domain](#), *Non. Anal. Real World Applications*, **14** (2013), 1755–1779.
- [10] A. Gierer and H. Meinhardt, [A theory of biological pattern formation](#), *Kybernetik*, **12** (1972), 30–39.
- [11] G. Hetzer, A. Madzvamuse and W. Shen, [Characterization of Turing diffusion-driven instability on evolving domains](#), *Disc. Con. Dyn. Sys.*, **32** (2012), 3975–4000.
- [12] M. Iida and M. Mimura, [Diffusion, cross-diffusion and a competitive interaction](#), *J. Math. Biol.*, **53** (2006), 617–641.
- [13] K. Korvasova, E. A. Gaffney, M. P. Maini, M. A. Ferreira and V. Klika, [Investigating the Turing conditions for diffusion-driven instability in the presence of binding immobile substrate](#), *J. Theor. Biol.*, **367** (2015), 286–295.
- [14] S. Kovács, [Turing bifurcation in a system with cross-diffusion](#), *Nonlinear Analysis*, **59** (2004), 567–581.
- [15] O. Lakkis, A. Madzvamuse and C. Venkataraman, [Implicit–explicit timestepping with finite element approximation of reaction–diffusion systems on evolving domains](#), *SIAM JNA*, **51** (2013), 2309–2330.
- [16] C. B. Macdonald, B. Merriman and S. J. Ruuth, [Simple computation of reaction-diffusion processes on point clouds](#), *Proc. Nat. Acad. Sci. USA.*, **110** (2013), 9209–9214.
- [17] C. B. Macdonald and S. J. Ruuth, [The implicit closest point method for the numerical solution of partial differential equations on surfaces](#), *SIAM J. Sci. Comput.*, **31** (2010), 4330–4350.
- [18] A. Madzvamuse, R. D. K. Thomas, P. K. Maini and A. J. Wathen, [A numerical approach to the study of spatial pattern formation in the ligaments of arcoid bivalves](#), *Bulletin of Mathematical Biology*, **64** (2002), 501–530.

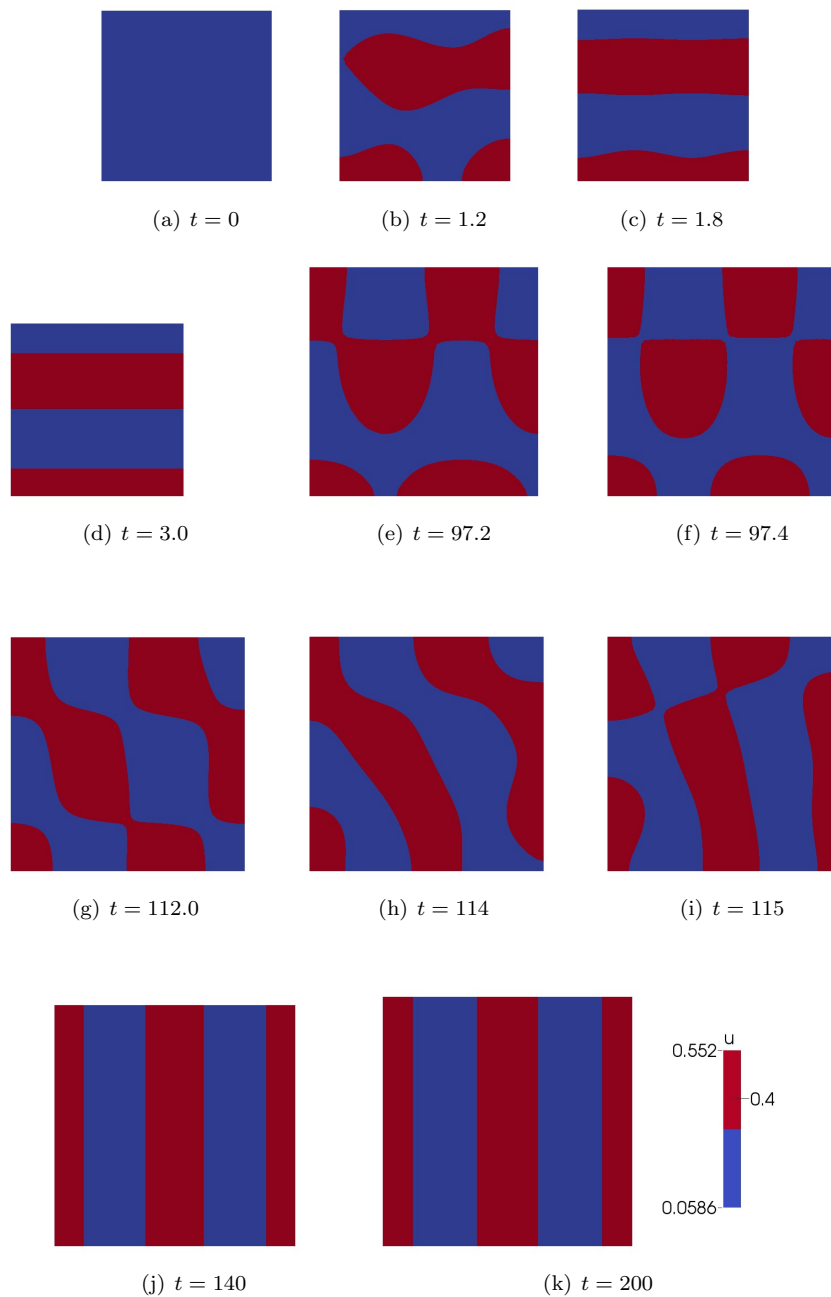


FIGURE 21. Numerical simulations corresponding to the chemical specie u with parameters $d = 0.5$, $a = 0.15$, $b = 0.15$, $d_u = -0.5$, $d_v = 0.8$ and $\gamma = 200$. Domain evolving of the unit square according to the logistic growth function with $r = 0.01$.

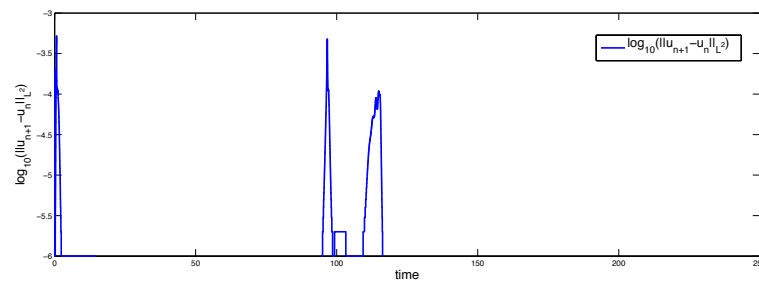
(a) $t = 0$

FIGURE 22. Plot of the evolution of the log of the L_2 -norm of the errors between successive numerical iterate solutions corresponding to patterns shown in Figure 21, for the case of logistic growth.

- [19] A. Madzvamuse, P. K. Maini and A. J. Wathen, [A moving grid finite element method applied to a model biological pattern generator](#), *J. Comp. Phys.*, **190** (2003), 478–500.
- [20] A. Madzvamuse, A. J. Wathen and P. K. Maini, [A moving grid finite element method for the simulation of pattern generation by Turing models on growing domains](#), *J. Sci. Comp.*, **24** (2005), 247–262.
- [21] A. Madzvamuse, [Time-stepping schemes for moving grid finite elements applied to reaction-diffusion systems on fixed and growing domains](#), *J. Sci. Phys.*, **214** (2006), 239–263.
- [22] A. Madzvamuse and M. K. Maini, [Velocity-induced numerical solutions of reaction-diffusion systems on fixed and growing domains](#), *J. Comp. Phys.*, **225** (2007), 100–119.
- [23] A. Madzvamuse, [Diffusion-driven instability for growing domains with divergence free mesh velocity](#), *Nonlinear Analysis: Theory, Methods and Applications*, **17** (2009), e2250–e2257.
- [24] A. Madzvamuse, E. A. Gaffney and M. K. Maini, [Stability analysis of non-autonomous reaction-diffusion systems: the effects of growing domains](#), *J. Math. Biol.*, **61** (2010), 133–164.
- [25] A. Madzvamuse and R. Barreira, [Exhibiting cross-diffusion-induced patterns for reaction-diffusion systems on evolving domains and surfaces](#), *Physical Review E*, **90** (2014), 043307, 14pp.
- [26] A. Madzvamuse, H. S. Ndakwo and R. Barreira, [Cross-diffusion-driven instability for reaction-diffusion systems: Analysis and simulations](#), *Journal of Math. Bio.*, **70** (2015), 709–743.
- [27] P. K. Maini, E. J. Crampin, A. Madzvamuse, A. J. Wathen and R. D. K. Thomas, [Implications of domain growth in morphogenesis](#), in *Mathematical Modelling and Computing in Biology and Medicine*, Capaso, V., ed., *Proceedings of the 5th European Conference for Mathematics and Theoretical Biology*: Conference, Milan, Italy. **1** (2003), 67–73.
- [28] M. S. McAfree and O. Annunziata, [Cross-diffusion in a colloid-polymer aqueous system](#), *Fluid Phase Equilibria*, **356** (2013), 46–55.
- [29] C. C. McCluskey, [A strategy for constructing Lyapunov functions for non-autonomous linear differential equations](#), *Linear Algebra and its Applications*, **409** (2005), 100–110.
- [30] J. D. Murray, *Mathematical Biology. II*, Volume 18 of Interdisciplinary Applied Mathematics. Springer-Verlag, New York. Third edition. Spatial models and biomedical applications, 2003.
- [31] R. G. Plaza, F. Sánchez-Garduño, P. Padilla, R. A. Barrio and P. K. Maini, [The effect of growth and curvature on pattern formation](#), *J. Dynam. and Diff. Eqs.*, **16** (2004), 1093–1121.
- [32] I. Prigogine and R. Lefever, [Symmetry breaking instabilities in dissipative systems. II](#), *J. Chem. Phys.*, **48** (1968), 1695–1700.
- [33] F. Rossi, V. K. Vanag, E. Tiezzi and I. R. Epstein, [Quaternary cross-diffusion in water-in-oil microemulsions loaded with a component of the Belousov-Zhabotinsky reaction](#), *J. Phys. Chem. B*, **114** (2010), 8140–8146.
- [34] R. Ruiz-Baier and C. Tian, [Mathematical analysis and numerical simulation of pattern formation under cross-diffusion](#), *Non. Anal. Real World Applications*, **14** (2013), 601–612.
- [35] J. Schnakenberg, [Simple chemical reaction systems with limit cycle behaviour](#), *J. Theor. Biol.*, **81** (1979), 389–400.

- [36] L. Z. Tian and M. Pedersen, [Instability induced by cross-diffusion in reaction-diffusion systems](#), *Non. Anal.: Real World Applications*, **11** (2010), 1036–1045.
- [37] A. Turing, On the chemical basis of morphogenesis, *Phil. Trans. Royal Soc. B*, **237** (1952), 37–72.
- [38] V. K. Vanag and I. R. Epstein, [Cross-diffusion and pattern formation in reaction diffusion systems](#), *Phys. Chem. Chem. Phys.*, **11** (2009), 897–912.
- [39] C. Venkataraman, O. Lakkis and A. Madzvamuse, [Global existence for semilinear reaction-diffusion systems on evolving domains](#), *Journal of Mathematical Biology*, **64** (2012), 41–67.
- [40] A. Vergara, F. Capuano, L. Paduano and R. Sartorio, Lysozyme mutual diffusion in solutions crowded by poly(ethylene glycol), *Macromolecules*, **39** (2006), 4500–4506.
- [41] Z. Xie, [Cross-diffusion induced Turing instability for a three species food chain model](#), *J. Math. Anal. and Appl.*, **388** (2012), 539–547.
- [42] J. F. Zhang, W. T. Li and Y. X. Wang, [Turing patterns of a strongly coupled predator-prey system with diffusion effects](#), *Non. Anal.*, **74** (2011), 847–858.
- [43] E. P. Zemskov, V. K. Vanag and I. R. Epstein, [Amplitude equations for reaction-diffusion systems with cross-diffusion](#), *Phys. Rev. E.*, **84** (2011), 036216.

Received January 2015; revised August 2015.

E-mail address: a.madzvamuse@sussex.ac.uk

E-mail address: H.Ndakwo@sussex.ac.uk

E-mail address: raquelbarreira@gmail.com